PERGAMON

Computers & Fluids 29 (2000) 813–847

computers & fluids

www.elsevier.com/locate/compfluid

A sequel to a rough Godunov scheme: application to real gases

Thierry Buffard[a,*], Thierry Gallouët[b], Jean-Marc Hérard[c]

[a]*Laboratoire de Mathématiques Appliquées, Université Blaise Pascal, 63177, Aubière Cedex, France*
[b]*Centre de Mathématiques et Informatique, Université de Provence, 39, rue Joliot Curie, 13453 Marseille Cedex 13, France*
[c]*Département Laboratoire National d'Hydraulique, Electricité de France, 6, Quai Watier 78401, Chatou Cedex, France*

Received 18 June 1998; received in revised form 4 January 1999; accepted 13 January 1999

Abstract

We present here an approximate Riemann solver to compute Euler equations using real gas state laws. The scheme is based on an earlier proposition, called VFRoe, introduced by one of the authors. It makes use of non conservative variables in order to preserve numerically Riemann invariants through the contact discontinuity. Detailed investigation of actual rate of convergence of the scheme is reported. The study also includes a comparison with original VFRoe and Roe schemes.

1. Introduction

We are interested in numerical solutions of initial-value hyperbolic systems of conservation laws:

$$\frac{\partial \mathbf{W}}{\partial t} + \frac{\partial \mathbf{F}(\mathbf{W})}{\partial x} = 0 \tag{1}$$

$$\mathbf{W}(x, 0) = \mathbf{W}_0(x) \tag{2}$$

* Corresponding author.
E-mail addresses: buffard@ucfma.univ-bpclermont.fr (T. Buffard), Thierry.Gallouet@umpa.ens-lyon.fr (T. Gallouët), Jean-Marc.Herard@der.edfgdf.fr (J.M. Hérard).

0045-7930/00/$ - see front matter
PII: S0045-7930(99)00026-2

where $\mathbf{W}(x, t) \in \mathbb{R}^p$ and the flux $\mathbf{F}(\mathbf{W})$ is such that the Jacobian matrix given by $\mathbf{A}(\mathbf{W}) = \frac{\partial \mathbf{F}}{\partial \mathbf{W}}$ is diagonalizable with real eigenvalues.

Finite volume schemes in conservation form have proven their efficiency to solve such problems. The most popular ones are based on the resolution of local Riemann problems at each interface. The first one, proposed by Godunov [1], is based on the exact solution of the one-dimensional Riemann problem associated with Eq. (1). It enjoys very good properties in the one-dimensional case (in particular, it fulfills the positivity of density and pressure for the Euler system) but its main drawbacks are its cost and its lack of robustness when the integration of Riemann invariants cannot be done analytically. Schemes based on Approximate Riemann solvers were introduced to avoid these difficulties. The commonly used Roe scheme [2] requires the knowledge of analytical eigenvalues and eigenvectors of the Jacobian matrix and, above all, the definition of a matrix of linearization $\mathbf{A}(W_L, W_R) \in M_p(\mathbb{R})$ such that:

$$\mathbf{A}(\mathbf{W}_L, \mathbf{W}_R) \quad \text{is diagonalizable with real eigenvalues} \tag{3}$$

$$\mathbf{F}(\mathbf{W}_R) - \mathbf{F}(\mathbf{W}_L) = \mathbf{A}(\mathbf{W}_L, \mathbf{W}_R)(\mathbf{W}_R - \mathbf{W}_L). \tag{4}$$

$$\mathbf{A}(\mathbf{W}, \mathbf{W}) = \frac{\partial \boldsymbol{F}(\mathbf{W})}{\partial \mathbf{W}}. \tag{5}$$

Remark that condition (5) may be replaced by: $\mathbf{A}$ is a continuous mapping of $\mathbb{R}^p \times \mathbb{R}^p$ in $M_p(\mathbb{R})$. The main losses in comparison with Godunov's scheme are the violation of the entropy law (a sonic entropy correction must be added), and, for instance, when dealing with the Euler system, the occurence of nonpositive density or pressure values. Moreover, finding a matrix satisfying Roe's condition (4) may sometimes be difficult or even impossible for some systems: Euler with real gas, some two-phase flow models and some complex turbulence models for example. This fact has motivated the development of an alternative to the Roe scheme. This simple Finite Volume scheme, called VFRoe, was introduced in Refs. [3–5] to approximate solutions of a two-phase flow model. Following the conservative approach of the Godunov scheme, the VFRoe flux function identifies with the physical one. As with the Roe scheme, the Riemann problems at each interface are linearized. Roe's condition is not necessary here, since one does not need to fulfill a consistency relation with the integral form of the conservation laws. Let us note two drawbacks of the VFRoe scheme, already finded with the Roe scheme: it admits entropy-violating stationary discontinuities, and it can produce nonpositive density or pressure values when it is applicated to the Euler system for example. Nonetheless, its behavior in many configurations is quite good and its application field is wider than Roe's one. Let us mention another approach recently considered in Ref. [6] for the resolution of a two phase flow in a pipe.

We propose here an extension of the VFRoe scheme: VFRoe using non conservative variables, noted here VFRoencv. Although it differs from VFRoe by the resolution of a linearized system written in non conservative variables, it may be used for smooth and non smooth flow. In this paper, the VFRoencv scheme is presented and tested on the Euler set of equations for equilibrium real gas with various equations of state (EOS). Many classical numerical schemes have been extended to include real-gas effects. Extensions of exact Riemann solver have been obtained by Collela and Glaz [7] (with a model based on an approximation of

γ across the waves), by Saurel et al. [8] and by Letellier and Forestier [9]. For equilibrium real gases, different approaches have been considered for generalized Roe average. Grossman and Walters [10] have introduced an equivalent γ to relate c^2 and h as in perfect gases. The more classical approach is to find $\bar{\chi}$ and $\bar{\kappa}$ satisfying $\Delta p = \bar{\chi}\Delta\rho + \bar{\kappa}\Delta\epsilon$ (or an equivalent form) so that relation (4) holds. Here, the greatest difficulty comes from the approximation of (generally pressure-) derivatives. Different formulas have been obtained by Glaister [11], Liou et al. [12], Vinokur and Montagné [13], Abgrall [14] in the case of chemically equilibrium flow, Toumi [15], Buffat and Page [16] who choose the temperature, instead of the pressure, as the relevant thermodynamic parameter. The 'simplest' extensions of the Roe scheme cannot be applied in practice if the EOS is a non-convex function for example, whereas others need the evaluation of integrals. A new technique using relaxation of energy allows the extension of classical approximate Riemann solvers used in perfect gas to treat real gases; it has been introduced by Coquel and Perthame [17], and tested by In [18]. The approach using a kinetic scheme has also been extended (see El Amine [19]) to non-isentropic real fluids. The VFRoencv scheme seems to be an interesting alternative according to numerical test cases presented here (see also Refs. [20,21]). It is a simple scheme, sometimes cheaper than previous ones.

In the next section, we briefly recall the Roe and Godunov schemes ([22]). Section 3 introduces the VFRoencv-type scheme on a general hyperbolic system (1). In Section 4, we propose a VFRoencv scheme when focusing on Euler equations. We also prove some relevant properties, especially in the case of ideal gas. We will discuss in Section 5 the results of several test cases, together with comparisons with other schemes when possible, for several equations of state. Extensions to second order, with the M.U.S.C.L. method and to multidimensional in space, are also presented in Section 6. An appendix is devoted to boundary conditions. In particular, a study in the case of rigid wall boundary condition with 'mirror state' technique is given (comparison between Godunov, Roe and VFRoencv approaches).

2. Finite volumes and Riemann solvers

First, we introduce some notations.

Let ε denote the set of $\mathbf{W}$ states such that system (1) is hyperbolic.

For the sake of simplicity, only regular meshes with constant spacing $\Delta x = x_{j+\frac{1}{2}} - x_{j-\frac{1}{2}}$ will be considered. We note $t^n = n\Delta t$ where Δt stands for the time step value. In the following, we shall describe Finite Volumes approximations $\mathbf{W}_j^n$ to weak solutions $\mathbf{W}$ of Eqs. (1) and (2) i.e. $\mathbf{W}_j^n$ is an approximation to $\frac{1}{\Delta x}\int_{x_{j-\frac{1}{2}}}^{x_{j+\frac{1}{2}}} \mathbf{W}(x, t^n)\,\mathrm{d}x$ defined by:

$$\mathbf{W}_j^0 = \frac{1}{\Delta x}\int_{x_{j-\frac{1}{2}}}^{x_{j+\frac{1}{2}}} \mathbf{W}_0(x)\,\mathrm{d}x, \quad j \in \mathbb{Z}$$

$$\mathbf{W}_j^{n+1} = \mathbf{W}_j^n - \frac{\Delta t}{\Delta x}\left(\boldsymbol{\Phi}^n_{j+\frac{1}{2}} - \boldsymbol{\Phi}^n_{j-\frac{1}{2}}\right), \quad j \in \mathbb{Z}, \quad n \in \mathbb{N} \tag{6}$$

where $\boldsymbol{\Phi}^n_{j+\frac{1}{2}}$ is the numerical flux at the interface $x_{j+\frac{1}{2}}$. Consider a three-point scheme:

$$\boldsymbol{\Phi}^n_{j+\frac{1}{2}} = \boldsymbol{\Phi}\left(\mathbf{W}^n_j, \mathbf{W}^n_{j+1}\right)$$

We require that the numerical flux is consistent with the physical flux in the sense (see [23,24]):

$$\forall \mathbf{U} \in \varepsilon, \qquad \boldsymbol{\Phi}(\mathbf{U}, \mathbf{U}) = \mathbf{F}(\mathbf{U}). \tag{7}$$

Recall that a Riemann problem in x_0 is a Cauchy problem (1) and (2) with initial condition:

$$\mathbf{W}_0(x) = \begin{cases} \mathbf{W}_L & \text{if } x < x_0 \\ \mathbf{W}_R & \text{if } x > x_0 \end{cases} \tag{8}$$

For given states $\mathbf{W}_L$ and $\mathbf{W}_R$, the entropy solution $\mathbf{W}(x, t)$ of Eqs. (1), (2) and (8), is a function of $\xi = \frac{x-x_0}{t}$, noted here $\mathbf{W}_{\text{exa}}(\xi;\mathbf{W}_L,\mathbf{W}_R)$.

For Riemann solvers, the numerical flux $\boldsymbol{\Phi}(\mathbf{U}, \mathbf{V})$ is obtained from the resolution of a Riemann problem with initial values $\mathbf{W}_L = \mathbf{U}$ and $\mathbf{W}_R = \mathbf{V}$.

2.1. Godunov's scheme

To compute the numerical approximation $\mathbf{W}^{n+1}_j$ (for $j \in \mathbb{Z}$) at time level t^{n+1}, starting from the approximation $\mathbf{W}^n_j$ (for $j \in \mathbb{Z}$), the basic idea of the Godunov scheme is the following: Riemann problems (1), (2) and (8) at each interface $x_{j+\frac{1}{2}}$ with $\mathbf{W}_L = \mathbf{W}^n_j$ and $\mathbf{W}_R = \mathbf{W}^n_{j+1}$ are solved exactly; assuming there is no interaction between two neighboring Riemann problems (CFL condition), $\mathbf{W}^{n+1}_j$ is obtained by averaging the latter solution at the time level t^{n+1} on $[x_{j-\frac{1}{2}}, x_{j+\frac{1}{2}}]$:

$$\mathbf{W}^{n+1}_j = \frac{1}{\Delta x}\int_0^{\Delta x/2} \mathbf{W}_{\text{exa}}\left(\frac{x}{\Delta t};\mathbf{W}^n_{j-1}, \mathbf{W}^n_j\right) \mathrm{d}x + \frac{1}{\Delta x}\int_{-\Delta x/2}^{0} \mathbf{W}_{\text{exa}}\left(\frac{x}{\Delta t};\mathbf{W}^n_j, \mathbf{W}^n_{j+1}\right) \mathrm{d}x. \tag{9}$$

Since we consider here the exact solution of Riemann problems associated with Eq. (1), we can evaluate the integral defining $\mathbf{W}^{n+1}_j$ and we get the Godunov scheme in conservation form (6) with:

$$\boldsymbol{\Phi}(\mathbf{U}, \mathbf{V}) = \mathbf{F}(\mathbf{W}_{\text{exa}}(\xi = 0;\mathbf{U}, \mathbf{V})) \tag{10}$$

We recall that, thanks to the Rankine–Hugoniot relation, the Godunov flux function defined by Eq. (10) is continuous (moreover, it is piecewise differentiable).

2.2. Roe's scheme

In 1983, Harten et al. [23] introduced a class of numerical schemes which includes the Godunov scheme. In Godunov-type schemes, the exact solution $\mathbf{W}_{\text{exa}}(\xi = \frac{x}{t};\mathbf{W}_L, \mathbf{W}_R)$ of the Riemann problem is replaced by an approximation $\mathbf{W}_{\text{app}}(\xi = \frac{x}{t};\mathbf{W}_L,\mathbf{W}_R)$ which fulfills:

(i) Consistency with the integral form of the conservation law

$$\int_{-\Delta x/2}^{\Delta x/2} \mathbf{W}_{\text{app}}\left(\frac{x}{\Delta t};\mathbf{W}_L,\mathbf{W}_R\right) \mathrm{d}x = \frac{\Delta x}{2}(\mathbf{W}_L + \mathbf{W}_R) + \Delta t(\mathbf{F}(\mathbf{W}_L) - \mathbf{F}(\mathbf{W}_R)) \tag{11}$$

(ii) Consistency with the integral form of the entropy condition

$$\int_{-\Delta x/2}^{\Delta x/2} \eta\left(\mathbf{W}_{\text{app}}\left(\frac{x}{\Delta t};\mathbf{W}_L,\mathbf{W}_R\right)\right) \mathrm{d}x \leq \frac{\Delta x}{2}\big(\eta(\mathbf{W}_L) + \eta(\mathbf{W}_R)\big) + \Delta t(G(\mathbf{W}_L) - G(\mathbf{W}_R)) \tag{12}$$

where (η, G) is an entropy–entropy flux pair for Eq. (1). The process to compute $\mathbf{W}_j^{n+1}$ remains unchanged ($\mathbf{W}_{\text{app}}$ replaces $\mathbf{W}_{\text{exa}}$ in Eq. (9)). However, except the Godunov numerical flux, Godunov-type fluxes cannot be written under the form:

$$\boldsymbol{\Phi}(\mathbf{U}, \mathbf{V}) = \mathbf{F}\big(\mathbf{W}_{\text{app}}(\xi = 0;\mathbf{U}, \mathbf{V})\big)$$

Roe's proposal [2], does not belong to this class of schemes, owing to the fact that it does not satisfy Eq. (12). The approximation $\mathbf{W}_{\text{app}}(\frac{x}{t};\mathbf{W}_L,\mathbf{W}_R)$ is obtained by the resolution of a linearized Riemann problem:

$$\begin{cases} \dfrac{\partial \mathbf{W}}{\partial t} + \mathbf{A}(\mathbf{W}_L, \mathbf{W}_R)\dfrac{\partial \mathbf{W}}{\partial x} = 0 \\ \mathbf{W}(x, 0) = \begin{cases} \mathbf{W}_L & \text{if } x < 0 \\ \mathbf{W}_R & \text{if } x > 0 \end{cases} \end{cases}$$

where the matrix $\mathbf{A}(\mathbf{W}_L, \mathbf{W}_R)$ satisfies conditions (3), (4) and (5). The second relation, called Roe's relation, is equivalent to the consistency relation with integral form of conservation law (11). Conservation form (6) of Roe's scheme finally leads to the following expression for the numerical flux:

$$\boldsymbol{\Phi}(\mathbf{U}, \mathbf{V}) = \frac{1}{2}\big(\mathbf{F}(\mathbf{U}) + \mathbf{F}(\mathbf{V}) - \big|\mathbf{A}(\mathbf{U}, \mathbf{V})\big|(\mathbf{V} - \mathbf{U})\big)$$

In practice, matrix $\mathbf{A}(\mathbf{W}_L, \mathbf{W}_R)$ is often determined using the assumption that there exists an average state $\tilde{\mathbf{W}}(\mathbf{W}_L, \mathbf{W}_R)$ such that:

$$\mathbf{A}(\mathbf{W}_L, \mathbf{W}_R) = \frac{\partial \mathbf{F}}{\partial \mathbf{W}}\big(\tilde{\mathbf{W}}(\mathbf{W}_L, \mathbf{W}_R)\big)$$

The average state of Roe $\tilde{\mathbf{W}}(\mathbf{W}_L, \mathbf{W}_R)$ must be in agreement with Eq. (4). Roe's average does not necessarily exist, or may not be unique (see, for example, [12]). Nethertheless, when system (1) has an entropy function, Harten [25] has established the existence of such a matrix.

3. VFRoencv scheme

3.1. General presentation

We present here the VFRoencv scheme for a general hyperbolic system in conservation form

(1). VFRoencv is a Finite Volume scheme, based on the resolution of linearized Riemann problems.

Considering the change of variables $\mathbf{W} \longmapsto \mathbf{Y}(\mathbf{W})$ ($\mathbf{Y}$ is a smooth invertible function), system (1) reads in non conservative form:

$$\frac{\partial \mathbf{Y}}{\partial t} + \mathbf{B}(\mathbf{Y})\frac{\partial \mathbf{Y}}{\partial x} = 0 \tag{13}$$

where $B(\mathbf{Y}) = (\mathbf{W}_{,\mathbf{Y}}(\mathbf{Y}))^{-1}\mathbf{A}(\mathbf{W}(\mathbf{Y}))\mathbf{W}_{,\mathbf{Y}}(\mathbf{Y})$.

Systems (1) and (13) are equivalent for smooth solutions.

At each interface, we solve the following linearized Riemann problem:

$$\frac{\partial \mathbf{Y}}{\partial t} + \mathbf{B}(\hat{\mathbf{Y}})\frac{\partial \boldsymbol{Y}}{\partial x} = 0 \tag{14}$$

$$\mathbf{Y}(x, 0) = \begin{cases} \mathbf{Y}_L = \mathbf{Y}(\mathbf{W}_L) \text{ if } x < 0 \\ \mathbf{Y}_R = \mathbf{Y}(\mathbf{W}_R) \text{ if } x > 0 \end{cases} \tag{15}$$

where $\hat{\mathbf{Y}}$ is an average state depending on $\mathbf{Y}_L$ and $\mathbf{Y}_R$, such that: $\mathbf{W}(\hat{\mathbf{Y}}) \in \varepsilon$, and $\hat{\mathbf{Y}}(\mathbf{Y}_L, \mathbf{Y}_R) = \mathbf{Y}$ if $\mathbf{Y}_L = \mathbf{Y}_R = \mathbf{Y}$. Let us note that eigenvalues $\tilde{\lambda}_i$ (for $i \in \{1, \ldots, p\}$) of the matrix $\mathbf{B}(\hat{\mathbf{Y}})$ are all real, and that $\mathbf{B}(\hat{\mathbf{Y}})$ is diagonalizable.

We briefly recall the resolution of the Riemann problem for a linear hyperbolic system. We consider the representation of $\mathbf{Y}_R - \mathbf{Y}_L$ in terms of the right eigenvectors $\tilde{\mathbf{r}}_i$ of $\mathbf{B}(\hat{\mathbf{Y}})$:

$$\mathbf{Y}_R - \mathbf{Y}_L = \sum_{i=1}^{p} \tilde{\alpha}_i \tilde{\mathbf{r}}_i$$

If $\tilde{\mathbf{l}}_i$, $i = 1, \ldots, p$, stand for the left eigenvectors of $\mathbf{B}(\hat{\mathbf{Y}})$, satisfying ${}^t\tilde{\mathbf{l}}_i \cdot \tilde{\mathbf{r}}_k = \delta_{ik}$, we have:

$$\tilde{\alpha}_i = {}^t\tilde{\mathbf{l}}_i \cdot (\mathbf{Y}_R - \mathbf{Y}_L)$$

Suppose that the eigenvalues $\tilde{\lambda}_i$ are arranged in a nondecreasing order. The solution of the Riemann problem (14) and (15) is composed of constant states separated by a fan of p characteristic lines (see Fig. 1):

$$\mathbf{Y}_{\text{app}}\left(\frac{x}{t}; \mathbf{Y}_L, \mathbf{Y}_R\right) = \begin{cases} \mathbf{Y}_0 = \mathbf{Y}_L & \text{if } x < \tilde{\lambda}_1 \, t \\ \mathbf{Y}_k = \mathbf{Y}_L + \displaystyle\sum_{i=1}^{k} \tilde{\alpha}_i \tilde{\mathbf{r}}_i & \text{if } \tilde{\lambda}_k t < x < \tilde{\lambda}_{k+1} t \quad \left(k \in \{1, \ldots, p-1\}\right) \\ \mathbf{Y}_p = \mathbf{Y}_R & \text{if } x > \tilde{\lambda}_p \, t \end{cases}$$

Then, if we suppose that no eigenvalue $\tilde{\lambda}_i$ vanishes, the approximate state, noted here $\mathbf{Y}^*_{LR}$, at the interface i.e. for $\frac{x}{t} = 0$, is given by:

$$\mathbf{Y}_{\text{app}}\left(\frac{x}{t}=0;\mathbf{Y}_L,\mathbf{Y}_R\right)=\mathbf{Y}_L+\sum_{\tilde{\lambda}_i<0}\tilde{\alpha}_i\tilde{\mathbf{r}}i=\mathbf{Y}_R-\sum_{\tilde{\lambda}_i>0}\tilde{\alpha}_i\tilde{\mathbf{r}}i \tag{16}$$

Finally, we define the conservative numerical flux by:

$$\boldsymbol{\Phi}(\mathbf{W}_L,\mathbf{W}_R)=\mathbf{F}\big(\mathbf{W}\big(\mathbf{Y}^*_{LR}\big)\big) \tag{17}$$

The approach, consisting in finding an approximate state to evaluate the physical flux, has also been considered in [26] for the Euler system.

3.2. Some remarks

The VFRoencv scheme needs to specify, the change of variable $\mathbf{W}\longmapsto\mathbf{Y}(\mathbf{W})$ on the one hand, and the average $\hat{\mathbf{Y}}$ on the other hand. The choices depend of course on the considered problem and may be guided by some desirable purposes. It may also be constrained to satisfy some desirable properties of the Riemann problem solution. The simplest average, which will be the one considered for the Euler system, is the arithmetic mean. In the case of $\mathbf{Y}(\mathbf{W})=\mathbf{W}$ (i.e. no change of variables), the corresponding scheme is the VFRoe scheme introduced in Ref. [3,4]. As regards numerical flux definition, VFRoencv schemes are inspired by the conservative form of the Godunov scheme. There is no L^2 projection step and no consistency with the integral form of the conservation law imposed for VFRoencv schemes. Of course, the matrix of linearization must satisfy Eq. (3) (in order to solve the Riemann problem) and Eq. (5) for some stability reason (upwinding of the scheme), but Roe's relation (4) is not necessary here.

The VFRoencv scheme is clearly conservative with consistent flux in the sense of Eq. (7).

If there exists $k\in\{1,\ldots,p\}$ such that $\tilde{\lambda}_k$ vanishes, fluxes on both sides of the interface are, a priori, different. The definition of a numerical flux, in this particular case, will be investigated for the Euler system.

As for Roe's scheme, the VFRoencv scheme admits a non physical weak solution, if the solution, for a genuinely non linear field, contains a rarefaction wave which crosses the

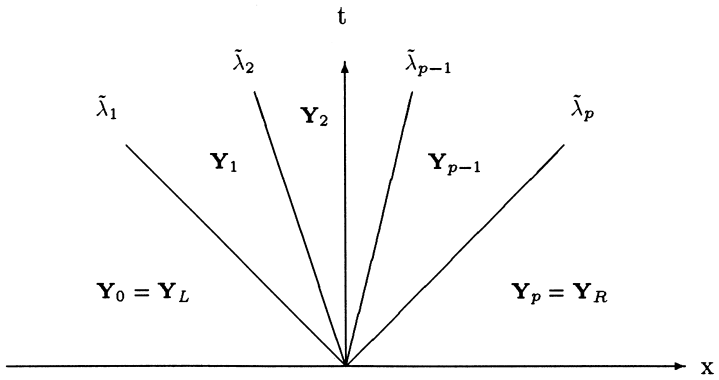

Fig. 1. Solution of the linearized Riemann problem.

interface. The sonic entropy correction considered here was described in an appendix to [27] by Harten and Hyman. The corresponding modification of the VFRoencv scheme is then the following. For a l-genuinely non linear field, suppose that:

$$\lambda_l(\mathbf{Y}_{l-1}) \leq 0 \leq \lambda_l(\mathbf{Y}_l) \quad \text{and} \quad \tilde{\lambda}_l \in \left[\lambda_l(\mathbf{Y}_{l-1}), \lambda_l(\mathbf{Y}_l)\right].$$

We introduce an intermediate state $\mathbf{Y}_m$ between $\mathbf{Y}_{l-1}$ and $\mathbf{Y}_l$ so that the initial discontinuity with speed $\tilde{\lambda}_l$ is replaced by two discontinuities with speed $\lambda_l(\mathbf{Y}_{l-1})$ and $\lambda_l(\mathbf{Y}_l)$:

$$(\lambda_l(\mathbf{Y}_l) - \lambda_l(\mathbf{Y}_{l-1}))\mathbf{Y}_m = \left(\lambda_l(\mathbf{Y}_l) - \tilde{\lambda}_l\right)\mathbf{Y}_l - \left(\tilde{\lambda}_l - \lambda_l(\mathbf{Y}_{l-1})\right)\mathbf{Y}_{l-1}$$

Finally, as the new solution contains $\mathbf{Y}_m$ at the interface, we define the numerical flux by Eq. (17), with $\mathbf{Y}^*_{LR} = \mathbf{Y}_m$.

4. Application to real gas Euler system

The conservation laws for the one-dimensional Euler equations for equilibrium real gases can be written in the form (1) with:

$$\mathbf{W} = \begin{bmatrix} \rho \\ \rho u \\ E \end{bmatrix}, \quad \mathbf{F}(\mathbf{W}) = \begin{bmatrix} \rho u \\ \rho u^2 + p \\ u(E+p) \end{bmatrix} \tag{18}$$

where $\rho(x,t)$, $u(x,t)$, $p(x,t)$, $E(x,t)$ respectively refer to the density, the velocity, the pressure and the total energy of the particular gas under consideration, at position x and time t. The total energy is defined by: $E = \rho(\epsilon + u^2/2)$, where ϵ is the internal energy per mass unit. We consider here ϵ as a function of the entropy S and of the specific volume $\tau(x, t) = \rho^{-1}$.

We define the pressure p and the temperature T by:

$$p = -\frac{\partial \epsilon}{\partial \tau}, \qquad T = \frac{\partial \epsilon}{\partial S}$$

The adiabatic exponent, given by:

$$\gamma = \frac{\tau}{p}\frac{\partial^2 \epsilon}{\partial \tau^2}$$

is a constant for ideal polytropic gases.

Finally, we introduce the sound speed, defined by:

$$c^2 = \tau^2 \frac{\partial^2 \epsilon}{\partial \tau^2}$$

We make appropriate assumptions on EOS so that system (1) and (18) is hyperbolic.

4.1. VFRoencv scheme in variable (τ, u, p)

For numerically solving the Euler set of equations, we suggest the VFRoencv scheme with:

$${}^t\mathbf{Y} = (\tau, u, p).$$

We can rewrite system (1) and (18), for smooth solutions, using these variables, in the following form:

$$\begin{cases} \dfrac{\partial \tau}{\partial t} + u\dfrac{\partial \tau}{\partial x} - \tau\dfrac{\partial u}{\partial x} = 0 \\ \dfrac{\partial u}{\partial t} + u\dfrac{\partial u}{\partial x} + \tau\dfrac{\partial p}{\partial x} = 0 \\ \dfrac{\partial p}{\partial t} + u\dfrac{\partial p}{\partial x} + \gamma p\dfrac{\partial u}{\partial x} = 0 \end{cases} \tag{19}$$

Hence, the VFRoencv scheme (in variable (τ, u, p)) is based on the linearized system (14) with:

$$\mathbf{Y} = \begin{pmatrix} \tau \\ u \\ p \end{pmatrix} \qquad \mathbf{B}(\hat{\mathbf{Y}}) = \begin{pmatrix} \hat{u} & -\hat{\tau} & 0 \\ 0 & \hat{u} & \hat{\tau} \\ 0 & \hat{\gamma}\hat{p} & \hat{u} \end{pmatrix} \tag{20}$$

We propose to take, for this linearization, the arithmetic mean: $\hat{\mathbf{Y}}(\mathbf{Y}_L, \mathbf{Y}_R) = \bar{\mathbf{Y}}(\mathbf{Y}_L, \mathbf{Y}_R)$ and $\hat{\gamma} = \bar{\gamma}$ where we use the following notation:

$$\bar{\varphi}(\mathbf{Y}_L, \mathbf{Y}_R) \overset{def}{=} \frac{\varphi(\mathbf{Y}_L) + \varphi(\mathbf{Y}_R)}{2}.$$

We introduce $\tilde{c}$ by $\tilde{c}^2 = \bar{\gamma}\bar{\tau}\bar{p}$. Eigenvalues of $\mathbf{B}(\bar{\mathbf{Y}})$ are given by:

$$\tilde{\lambda}_1 = \bar{u} - \tilde{c}, \quad \tilde{\lambda}_2 = \bar{u}, \quad \tilde{\lambda}_3 = \bar{u} + \tilde{c},$$

and the associated right eigenvectors by:

$$\tilde{\mathbf{r}}_1 = \begin{bmatrix} \bar{\tau} \\ \tilde{c} \\ -\bar{\gamma}\bar{p} \end{bmatrix}, \quad \tilde{\mathbf{r}}_2 = \begin{bmatrix} 1 \\ 0 \\ 0 \end{bmatrix}, \quad \tilde{\mathbf{r}}_3 = \begin{bmatrix} \bar{\tau} \\ -\tilde{c} \\ -\bar{\gamma}\bar{p} \end{bmatrix}$$

After some algebraic calculations we obtain the following expression for coefficients $\tilde{\alpha}_1$ and $\tilde{\alpha}_3$:

$$\tilde{\alpha}_1 = \frac{1}{2\tilde{c}^2}\left(\tilde{c}\Delta(u) - \bar{\tau}\Delta(p)\right)$$

$$\tilde{\alpha}_3 = -\frac{1}{2\tilde{c}^2}\left(\tilde{c}\Delta(u) + \bar{\tau}\Delta(p)\right)$$

where $\Delta(\cdot) = (\cdot)_R - (\cdot)_L$.

The intermediate states are then given by:

$$\mathbf{Y}_1 = \begin{bmatrix} \tau_1 \\ u_1 \\ p_1 \end{bmatrix} = \begin{bmatrix} \tau_L + \tilde{\alpha}_1 \bar{\tau} \\ u_L + \tilde{\alpha}_1 \tilde{c} \\ p_L - \tilde{\alpha}_1 \bar{\gamma} \bar{p} \end{bmatrix}, \quad \mathbf{Y}_2 = \begin{bmatrix} \tau_2 \\ u_2 \\ p_2 \end{bmatrix} = \begin{bmatrix} \tau_R - \tilde{\alpha}_3 \bar{\tau} \\ u_R + \tilde{\alpha}_3 \tilde{c} \\ p_R + \tilde{\alpha}_3 \bar{\gamma} \bar{p} \end{bmatrix} \tag{21}$$

We deduce the approximate state $\mathbf{Y}^*_{LR}$ at the interface used to determine the numerical flux by (17).

4.2. Some properties of the scheme

Property 1 deals with Riemann invariants associated with a linearly degenerate field. Recall that, for the Euler system (1) and (18), the only linearly degenerate field is the one associated with λ_2. The pair of 2-Riemann invariants can be taken as $\{u, p\}$.

Property 1.

(i) The solution of the linearized Riemann problem in variable (τ, u, p) satisfies: the 2-Riemann invariants u and p are constant across the 2-wave.
(ii) We assume that the EOS is such that $\rho\epsilon(\tau, S)$ is a (one-to-one) function of p. If the initial state $\mathbf{W}_0$ is such that the 2-Riemann invariants u and p are constant, then their values are not modified by the VFRoencv (τ, u, p) scheme (which identifies with the Godunov scheme).

Proof.

(i) Because of the last two null components of $\tilde{\mathbf{r}}_2$, we have $u_1 = u_2$ and $p_1 = p_2$ in formulas (21).
(ii) At each interface, under condition $\Delta(u) = \Delta(p) = 0$, we have: $\tilde{\alpha}_1 = \tilde{\alpha}_3 = 0$, hence $\mathbf{Y}_1 = \mathbf{Y}_L$ and $\mathbf{Y}_2 = \mathbf{Y}_R$.

If $u = u_L = u_R = 0$, although $\mathbf{Y}^*$ is not defined, we have ${}^t\mathbf{F}(\mathbf{W}(\mathbf{Y}_L)) = {}^t\mathbf{F}(\mathbf{W}_L) = {}^t\mathbf{F}(\mathbf{W}_R) = (0, p, 0)$. So, if we take $\boldsymbol{\Phi}(\mathbf{W}_L, \mathbf{W}_R) = \mathbf{F}(\mathbf{W}_L) = \mathbf{F}(\mathbf{W}_R)$ (this is in accordance with the definition of the numerical flux following Property 2 in the case of vanishing eigenvalue), the initial state $\mathbf{W}_0$ is a steady solution for the scheme.

Assuming now that $u = u_L = u_R > 0$ provides $\mathbf{Y}^* = \mathbf{Y}_L$ and the numerical flux reads:

$$\mathbf{F}(\mathbf{W}(\mathbf{Y}^*)) = \mathbf{F}(\mathbf{W}(\mathbf{Y}_L)) = \mathbf{F}(\mathbf{W}_L)$$

i.e. it identifies with Godunov's.

So, in a cell Ω_i, as we have $u_{i+1} = u_i = u_{i-1} = u$ and $p_{i+1} = p_i = p_{i-1} = p$, the first iteration in time for a general EOS yields:

$$\begin{cases} \rho_i^1 = \rho_i^0 - u\dfrac{\Delta t}{\Delta x}\Delta_{i-1/2}(\rho) \\ (\rho_i u_i)^1 = \rho_i^0 u - u^2\dfrac{\Delta t}{\Delta x}\Delta_{i-1/2}(\rho) \\ \left(\rho_i \epsilon(\tau, S)_i + \dfrac{1}{2}\rho_i u_i^2\right)^1 = \rho_i^0 \epsilon(\tau, S)_i^0 + \dfrac{1}{2}\rho_i^0 u^2 - u\dfrac{\Delta t}{\Delta x}\left(\Delta_{i-1/2}\big(\rho\epsilon(\tau, S)\big) + \dfrac{1}{2}u^2\Delta_{i-1/2}(\rho)\right) \end{cases}$$

where $\Delta_{i-1/2}(\varphi) = \varphi_i^0 - \varphi_{i-1}^0$.

We obtain, independently of the EOS: $u_i^1 = u$.

Finally, with the hypothesis on the EOS, the three previous equalities given by the scheme lead to: $p_i^1 = p$. So, u and p remain constant.

The hypothesis on the EOS is satisfied, in particular, for an ideal polytropic gas for which γ is constant and:

$$\epsilon(\tau, S) = \frac{p}{(\gamma - 1)\rho}. \tag{22}$$

This is no longer true, for example, with the EOS of Van der Waals. However, the VFRoencv flux identifies with Godunov's one regardless of this hypothesis. Notice that property 1 is true regardless of the particular choice for the average. A scheme satisfying (ii) for a Stiffened gas EOS is also presented in [28].

With the previous choices of $\mathbf{Y}$ and of the average, we have the following property concerning the behavior of the linearized system across one single wave of discontinuity.

We note $[\varphi]$ the jump of φ across one curve of discontinuity, and σ the speed of the discontinuity.

Property 2. For an ideal polytropic gas, exact jump relations (i.e. Rankine Hugoniot relations) of system (1) and (18):

$$-\sigma[\mathbf{W}] + \big[\mathbf{F}(\mathbf{W})\big] = 0 \tag{23}$$

and jump relations of system (14) and (20):

$$-\sigma[\mathbf{Y}] + \mathbf{B}(\bar{\mathbf{Y}})[\mathbf{Y}] = 0 \tag{24}$$

are equivalent.

We will use this property to define the VFRoencv flux for a steady discontinuity.

Remark 1. *We point out that this property* ***does not imply*** *the consistency relation with the integral form of the conservation law* (11) *for system* (1) *and* (18).

Proof. A convenient form of Rankine Hugoniot relations (23) for the system (1) and (18) is, by introducing the variable $v = u - \sigma$:

$$\begin{cases} [\rho v] = 0 & \text{(25a)} \\ \big[\rho v^2 + p\big] = 0 & \text{(25b)} \\ \left[v\left(\rho\epsilon(\tau, S) + \frac{1}{2}\rho v^2 + p\right)\right] = 0. & \text{(25c)} \end{cases}$$

Under the hypothesis that the gas is ideal polytropic, $\epsilon(\tau, S)$ satisfies Eq. (22).

Approximate jump relations (24) read:

$$\begin{cases} \bar{v}[\tau] - \bar{\tau}[v] = 0 & (26a) \\ \bar{v}[v] + \bar{\tau}[p] = 0 & (26b) \\ \bar{v}[p] + \gamma\bar{p}[v] = 0 & (26c) \end{cases}$$

We begin by recalling the following identity for all scalar variables φ and ψ:

$$[\varphi\psi] = \bar{\varphi}[\psi] + \bar{\psi}[\varphi]$$

We obtain equivalence between the two jump relations (25a) and (26a) corresponding to mass equation, thanks to the following equalities: $[\rho] = -\rho_L\rho_R[\tau]$ and : $\bar{\rho} = \rho_L\rho_R\bar{\tau}$.

Eq. (26b) is equivalent to:

$$\frac{1}{2\bar{\tau}}[v^2] + [p] = 0$$

Using Eq. (25a) leads to:

$$\frac{1}{2\bar{\tau}}[v^2] = [\rho v^2],$$

and consequently Eqs. (25a)–(25b), and Eqs. (26a)–(26b) are equivalent.

Finally, using Eq. (25b), the Eq. (26c) becomes:

$$\frac{\gamma}{\gamma - 1}[pv] + \bar{v}[\rho v^2] = 0$$

where, thanks to Eq. (25a):

$$\bar{v}[\rho v^2] = \frac{1}{2}[\rho v^3]$$

Substituting and considering γ constant, we obtain Eq. (25c).

Remark 2. *This result can be related with the works of De Vuyst* [29] *in the sense that we have equivalence between Rankine Hugoniot relations of* (1) *and* (18), *and jump relations of the non conservative system* (13), *represented by a linear path with respect to* (τ, u, p).

Remark 3. *In the case of a general EOS, Property 2 is still true if we take:*,

$$\hat{\gamma} = 1 + \frac{[p\tau]}{[\epsilon(\tau, S)]}.$$

Note that, for an ideal polytropic gas, this expression reduces to $\hat{\gamma} = \gamma$. *However, this expression not only may be undefined but its value may also lie outside its admissible range. For these reasons, we do not hold this definition of* $\hat{\gamma}$ *for the linearization.*

A consequence of Property 2 (when γ is constant) determines the behavior of the VFRoencv

scheme in variable (τ, u, p) with the choice of average $\hat{\mathbf{Y}} = \bar{\mathbf{Y}}$ in the case of a single stationary discontinuity:

$$\mathbf{W}_0(x) = \begin{cases} \mathbf{W}_L & \text{if } x < x_0 \\ \mathbf{W}_R & \text{if } x > x_0 \end{cases}, \quad \text{with } \mathbf{F}(\mathbf{W}_L) = \mathbf{F}(\mathbf{W}_R) \tag{27}$$

The initial condition $\mathbf{W}_0$ defined by Eq. (27) is indeed a steady entropy solution of (1), (2) and (18) if and only if the entropy condition: $G(\mathbf{W}_R) \leq G(\mathbf{W}_L)$ is fulfilled.

Thanks to Property 2, $[\mathbf{Y}]$ is an eigenvector of the matrix $\mathbf{B}(\bar{\mathbf{Y}})$ associated with a null eigenvalue. The solution of the linearized Riemann problem (14) and (20) with the initial condition (15) and (27) consists of two states $\mathbf{Y_L}$ and $\mathbf{Y}_R$ separated by the characteristic lines $\frac{x}{t} = 0$. We define, in this case, the VFRoencv flux by taking $\mathbf{Y}^*_{LR} = \mathbf{Y}_L$ or $\mathbf{Y}^*_{LR} = \mathbf{Y}_R$, so as to have an exact resolution of a single stationary discontinuity with the scheme for an ideal polytropic gas.

Note that the numerical flux defined above is continuous in this case. We also remark that the function defined by Eq. (27) is a steady solution of the basic VFRoencv scheme (i.e. without entropy correction) whether or not the entropy condition is satisfied.

We will use this property and Property 1 to suggest a definition of the numerical flux when a numerical eigenvalue $\tilde{\lambda}_k$ vanishes.

1. Suppose $k = 2$ (the associated field is linearly degenerate). The interface $\frac{x}{t} = 0$ separates the intermediate states $\mathbf{Y}_1$ and $\mathbf{Y}_2$. If $u_1 = u_2 = 0$, we have $\mathbf{F}(\mathbf{W}(\mathbf{Y}_1)) = \mathbf{F}(\mathbf{W}(\mathbf{Y}_2))$ (see Property 1), and we take $\boldsymbol{\Phi}(\mathbf{W}_L, \mathbf{W}_R) = \mathbf{F}(\mathbf{W}(\mathbf{Y}_1))$. Otherwise, we define $\mathbf{Y}^*_{LR} = \mathbf{Y}_1$ or $\mathbf{Y}^*_{LR} = \mathbf{Y}_2$ according to the sign of $u_1 = u_2$.
2. Suppose $k = 1$ (the associated field is genuinely nonlinear). The interface $\frac{x}{t} = 0$ separates the intermediate states $\mathbf{Y}_L$ and $\mathbf{Y}_1$. If γ is constant and if we have $\mathbf{Y}_1 = \mathbf{Y}_2 = \mathbf{Y}_R$, then the states $\mathbf{Y}_L$ and $\mathbf{Y}_R$ correspond to a single stationary discontinuity. So we take $\boldsymbol{\Phi}(\mathbf{W}_L, \mathbf{W}_R) = \mathbf{F}(\mathbf{W}(\mathbf{Y}_L)) = \mathbf{F}(\mathbf{W}(\mathbf{Y}_R))$. Otherwise, we define the numerical flux as the physical flux function calculated from the arithmetic mean state between the two neighboring intermediate states $\mathbf{Y}_L$ and $\mathbf{Y}_1$. The case $k = 3$ is similar.

We consider the numerical resolution of a Riemann problem whose solution is composed of a stationary 1-shock followed by a 2-contact discontinuity and a 3-rarefaction wave. The gas is an ideal polytropic one with $\gamma = 1.4$. The constant states of the solution are:

$$\begin{bmatrix} \rho_L \\ u_L \\ p_L \end{bmatrix} = \begin{bmatrix} 1 \\ 2 \\ 1 \end{bmatrix}, \quad \begin{bmatrix} \rho_1 \\ u_1 \\ p_1 \end{bmatrix} = \begin{bmatrix} 24/11 \\ 11/12 \\ 19/6 \end{bmatrix}, \quad \begin{bmatrix} \rho_2 \\ u_2 \\ p_2 \end{bmatrix} = \begin{bmatrix} 2^{2/7} \\ 11/12 \\ 19/6 \end{bmatrix}, \quad \begin{bmatrix} \rho_R \\ u_R \\ p_R \end{bmatrix} = \begin{bmatrix} 2 \\ u_R \\ 19/3 \end{bmatrix}$$

with: $u_R = u_1 - \frac{2}{\gamma - 1}(c_2 - c_R)$. The results by the VFRoencv scheme are displayed in Fig. 3, where one circle corresponds to one cell. The mesh is composed of 500 cells. The stationary 1-shock is, in this case, represented exactly. Roe's scheme, which solves exactly single stationary discontinuities, leads to similar results.

The question addressed in the following is whether the VFRoencv scheme keeps the variables within their physical (or mathematical) range. About this property, let us cite the study on positivity of the density in [30] in the case of ideal polytropic gas.

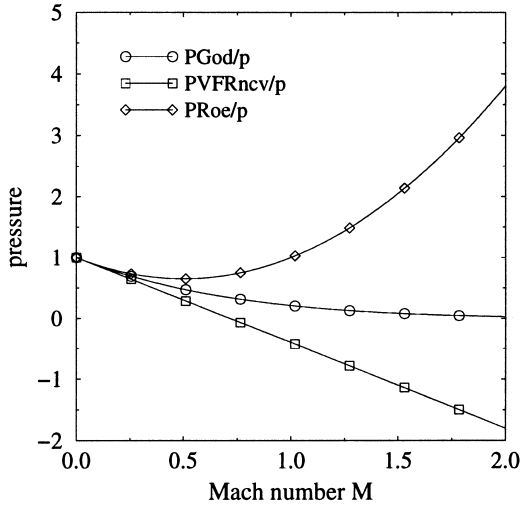

Fig. 2. Rigid wall pressure values.

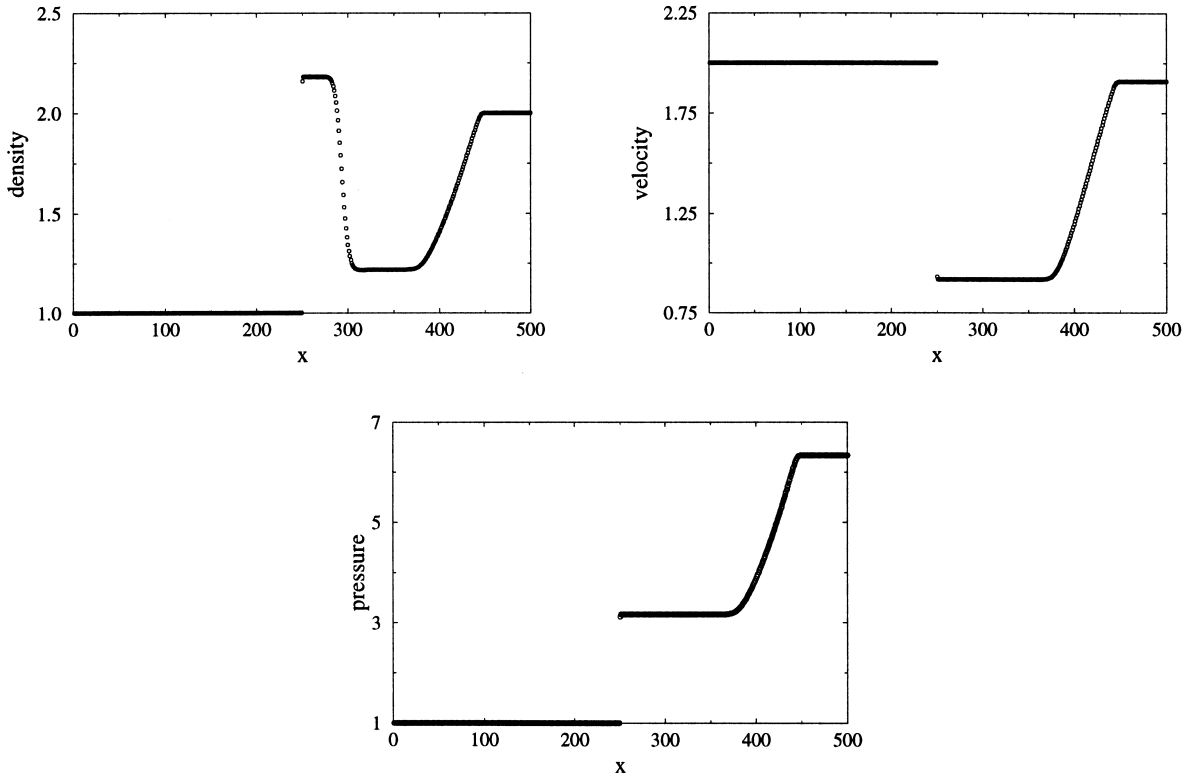

Fig. 3. Stationary l-shock.

We first recall that the Riemann problem, associated to the Euler system (1) and (18), has a unique entropy-consistent solution (we consider here c as a function of ρ and S) if and only if:

$$u_R - u_L < \int_0^{\rho_R} \frac{c(\rho,S_R)}{\rho}\,\mathrm{d}\rho + \int_0^{\rho_L} \frac{c(\rho,S_L)}{\rho}\,\mathrm{d}\rho$$

Otherwise, vacuum appears in the solution.

For an ideal polytropic gas (see Ref. [31]), we have:

$$\int_0^n \frac{c(\tau,S)}{\tau}\,\mathrm{d}\tau = \frac{2}{\gamma-1}c(\rho,S)$$

The VFRoencv scheme in variable $(\tau,\ u,\ p)$ with $\hat{\mathbf{Y}} = \bar{\mathbf{Y}}$ and $\hat{\gamma} = \bar{\gamma}$ leads to the following expression for the intermediate pressure:

$$p_1 = p_2 = \bar{p} - \frac{\tilde{c}(\bar{\gamma},\bar{p},\bar{\tau})}{2\bar{\tau}}\Delta(u)$$

(recall $\tilde{c}^2 = \bar{\gamma}\bar{p}\bar{\tau}$) or equivalently, in a more convenient form:

$$p_1 = p_2 = \frac{\tilde{c}}{\bar{\gamma}\bar{\tau}}\left(\tilde{c} - \frac{\bar{\gamma}}{2}\Delta(u)\right)$$

Thus, intermediate pressure is positive if and only if:

$$\Delta(u) < \frac{2}{\bar{\gamma}}\tilde{c}(\bar{\gamma},\bar{p},\bar{\tau}) \tag{28}$$

This condition applied to an ideal polytropic gas with $p_L = p_R$ and $\tau_L = \tau_R$ reads:

$$\Delta(u) < \frac{2}{\gamma}c$$

which is more restrictive than the 'continuous' condition:

$$\Delta(u) < \frac{4}{\gamma-1}c$$

Concerning the specific volume, we have the following expressions:

$$\tau_1 = \tau_L - \frac{\bar{\tau}}{2\bar{\gamma}\bar{p}}\Delta(p) + \frac{\bar{\tau}}{2\tilde{c}}\Delta(u)$$

or equivalently:

$$\tau_1 = \tau_L + \frac{\bar{\tau}}{2\tilde{c}}\left(\Delta(u) - \frac{\bar{\tau}}{\tilde{c}}\Delta(p)\right)$$

and with a similar calculation:

$$\tau_2 = \tau_R + \frac{\bar{\tau}}{2\bar{c}}\left(\Delta(u) + \frac{\bar{\tau}}{\bar{c}}\Delta(p)\right)$$

It is not easy to give explicit conditions on the specific volume positivity.

Remark 4. *Another property of the VFRoencv scheme, which is of interest to engineers, is the preservation of the total enthalpy H in stationary flows. It is satisfied here for 'interface' values of H.*

Indeed, the total enthalpy is given by: $H = (E + p)/\rho$ and let us denote by Q the momentum i.e. $Q = \rho u$. For stationary flows, the following relations hold for any j in $\mathbb{Z}$:

$$\begin{cases} Q^*_{j-\frac{1}{2}} = Q^*_{j+\frac{1}{2}} \\ Q^*_{j-\frac{1}{2}} H^*_{j-\frac{1}{2}} = Q^*_{j+\frac{1}{2}} H^*_{j+\frac{1}{2}} \end{cases}.$$

hence,

$$H^*_{j-\frac{1}{2}} = H^*_{j+\frac{1}{2}}$$

We insist that this is valid for 'interface' values only (and not for averaged values $H_j = H(\rho_j, Q_j, E_j)$)(see [30] for a scheme satisfying this property).

5. Numerical experiments (one-dimensional shock tubes)

We present numerical tests on shock tubes, for the three basic configurations: rarefaction–rarefaction, rarefaction–shock (shock–rarefaction is a similar configuration), and shock–shock. The computation domain consists of a one-dimensional tube with a membrane in the middle, which separates two different fluid states. All meshes used to solve these Riemann problems are regular.

We have considered three different EOS and carried out comparisons with other schemes.

5.1. Ideal polytropic gas

The EOS may be given by:

$$p = (\gamma - 1)\left(E - \frac{\rho u^2}{2}\right)$$

where the constant γ is equal to 1.4 (diatomic gas).

The CFL number here is equal to 0.7. For qualitative study, we present profiles for density, velocity and pressure. From a quantitative point of view, numerical convergence curves, at a given time, are represented by the logarithm of the relative L1-error as a function of the logarithm of the mesh size. The grids used contain 250, 500, 1000, 2000, 4000, 8000 (and

16000, 32000 for Sod shock tube) cells. A similar study with the VFRoe scheme can be found in [5]. The Riemann problems associated with the last two tests occur in the treatment of rigid wall boundary conditions with the 'mirror state' technique. In Appendix A, we will compare the interface pressures obtained with the Godunov, VFRoe and VFRoencv schemes.

5.1.1. Test 1: Sod shock tube

Initial conditions are given by:

$$(\rho_L, u_L, p_L) = \left(1, 0, 10^5\right)$$

$$(\rho_R, u_R, p_R) = \left(0.125, 0, 10^4\right)$$

The exact solution is composed of a 1-rarefaction wave followed by a 2-contact discontinuity and by a 3-shock. Profiles are given in Fig. 4 for a mesh of 500 cells, and convergence curves in Fig. 5. We note a small loss of monotonicity at the end of the rarefaction wave on density and pressure variables. The numerical rates of convergence are about 0.65 for density and

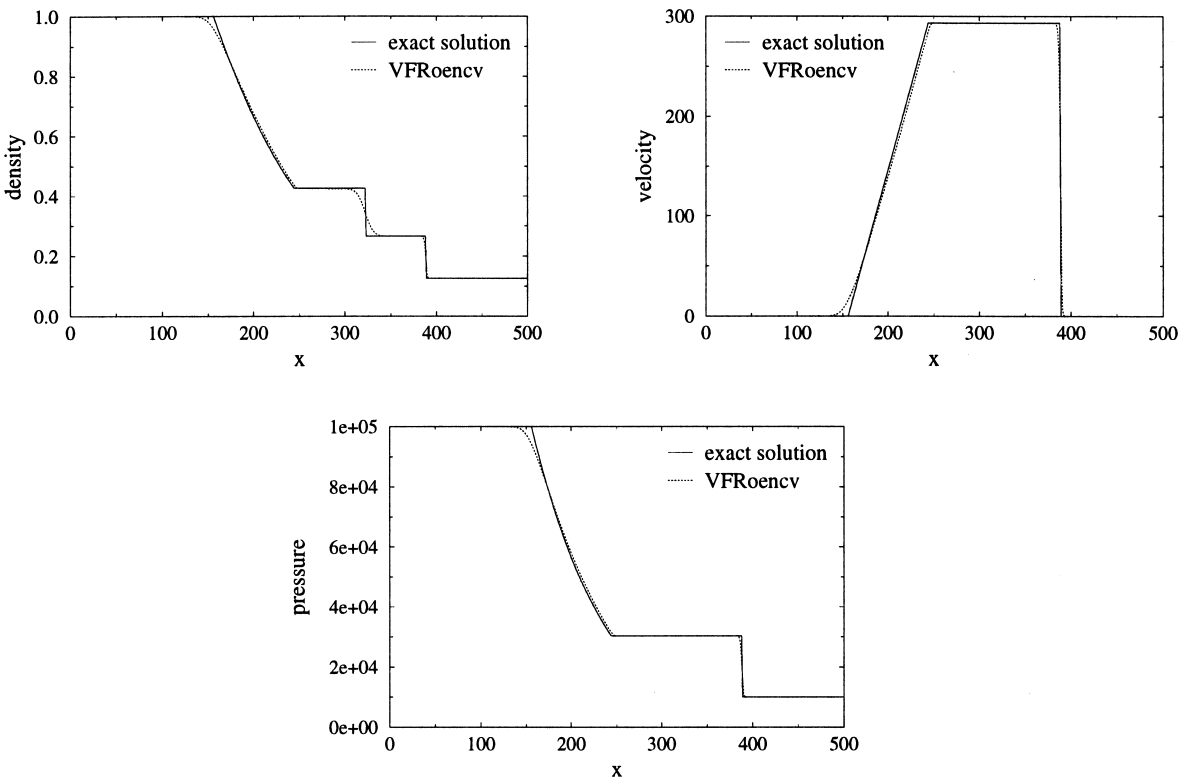

Fig. 4. Sod's shock tube.

slightly greater than 0.8 for velocity and pressure. The results are similar to the ones obtained with Roe or VFRoe schemes.

5.1.2. Test 2: supersonic shock tube

We increase the initial pressure ratio of p_L to p_R:

$$(\rho_L, u_L, p_L) = \left(5, 0, 5 \times 10^5\right)$$

$$(\rho_R, u_R, p_R) = \left(0.125, 0, 10^4\right)$$

The exact solution is composed of a 1-rarefaction wave presenting a sonic point followed by a 2-contact discontinuity and a 3-shock. As for Roe and VFRoe schemes, sonic entropy correction must be added to eliminate the stationary shock which appears at the sonic point. The small kink at the sonic point (see Fig. 6 for 500 cells) still exists, as with the Roe and VFRoe schemes, but vanishes on finer grids. The rates of convergence plotted on Fig. 7(a) are sligtly lower than in the previous test and less regular for the velocity (as with the Roe and VFRoe schemes). A slight difference between these schemes can be seen in this test case on the curve of convergence (see Fig. 7(b) for the pressure variable).

5.1.3. Test 3: symmetric double rarefaction

We now present two test cases whose solution, composed of two symmetric rarefaction waves, involves a state near vacuum. Given $u > 0$, we consider the initial conditions:

$$(\rho_L, u_L, p_L) = \left(1, -u, 10^5\right)$$

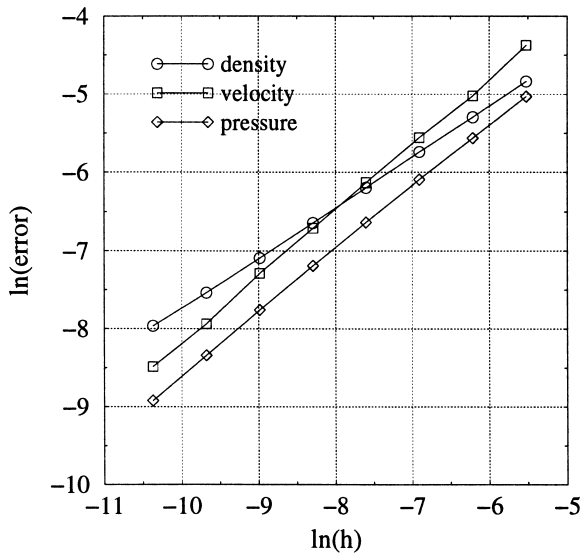

Fig. 5. L1 convergence curve for shock tube of Sod.

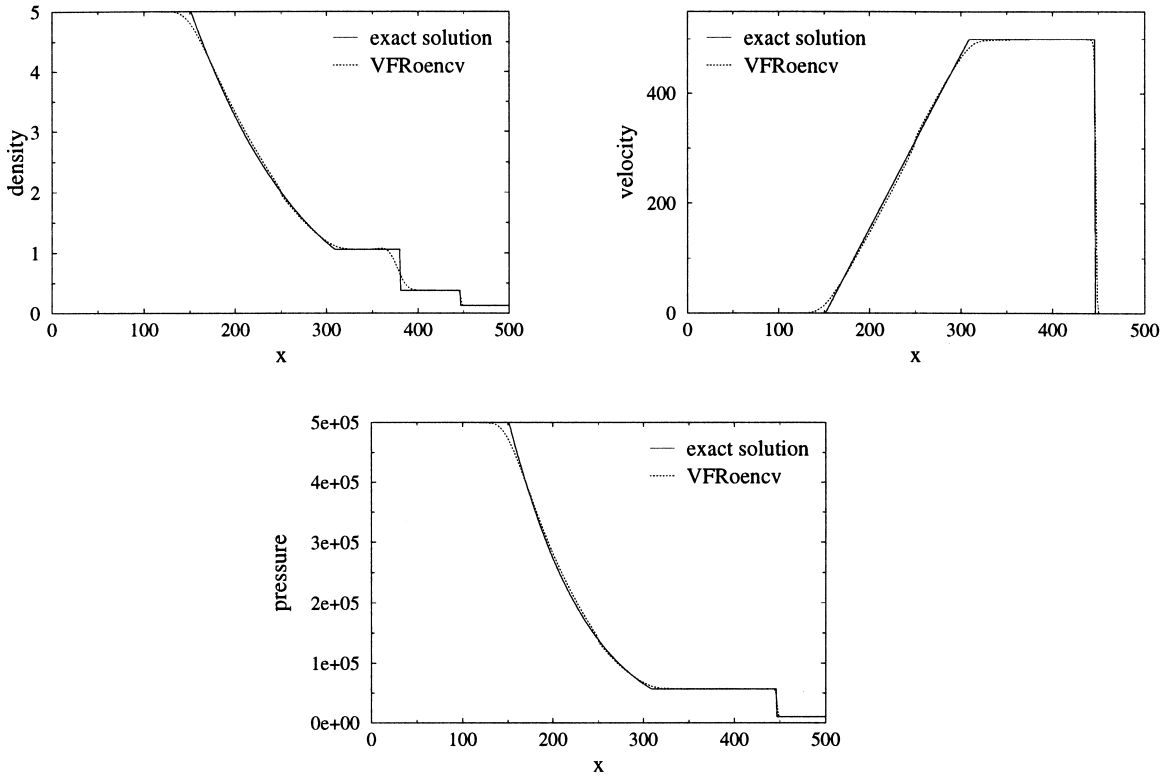

Fig. 6. Supersonic shock tube.

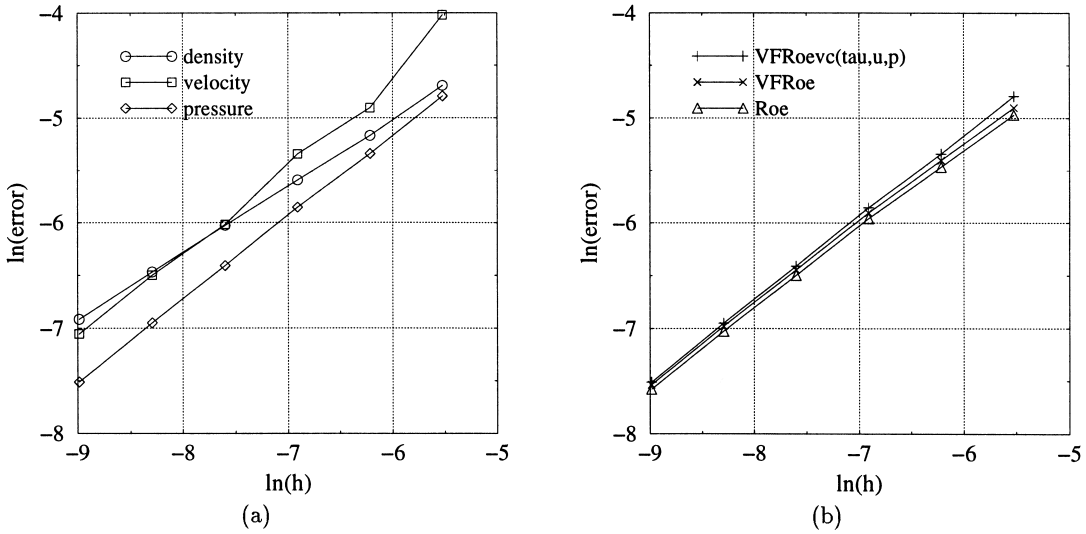

Fig. 7. L1 convergence curve for supersonic shock tube: (a) with VFRoencv scheme. (b) for pressure variable.

$$(\rho_R, u_R, p_R) = \left(1, u, 10^5\right)$$

First, we take: $u = 300$ so that the initial Mach number is less than one. We remark the classical drawback of Godunov-type schemes on the density variable near the position of initial discontinuity. The approximation of the rarefaction waves is correct (see Fig. 8 for a mesh of 1000 cells). The rate of convergence is the same for the three variables (about 0.78, see Fig. 9). The length of the 'stalactite' is a bit different depending on the scheme. Concerning the curves of convergence, comparison between the three schemes leads to similar remarks as for the previous test.

We consider the same test case with $u = 1200$. The initial Mach number is about 3.2 (for $\gamma = 1.4$, we recall that the limit of the initial Mach number for the solution of such a problem without vacuum is 5.). Let us note that in this case, the standard Roe and VFRoe schemes lead to negative values for pressure. For the VFRoencv scheme, we notice in Fig. 10 (500 cells) that the 'stalactite' is now less important and that the numerical minimum of the density becomes greater than the exact value.

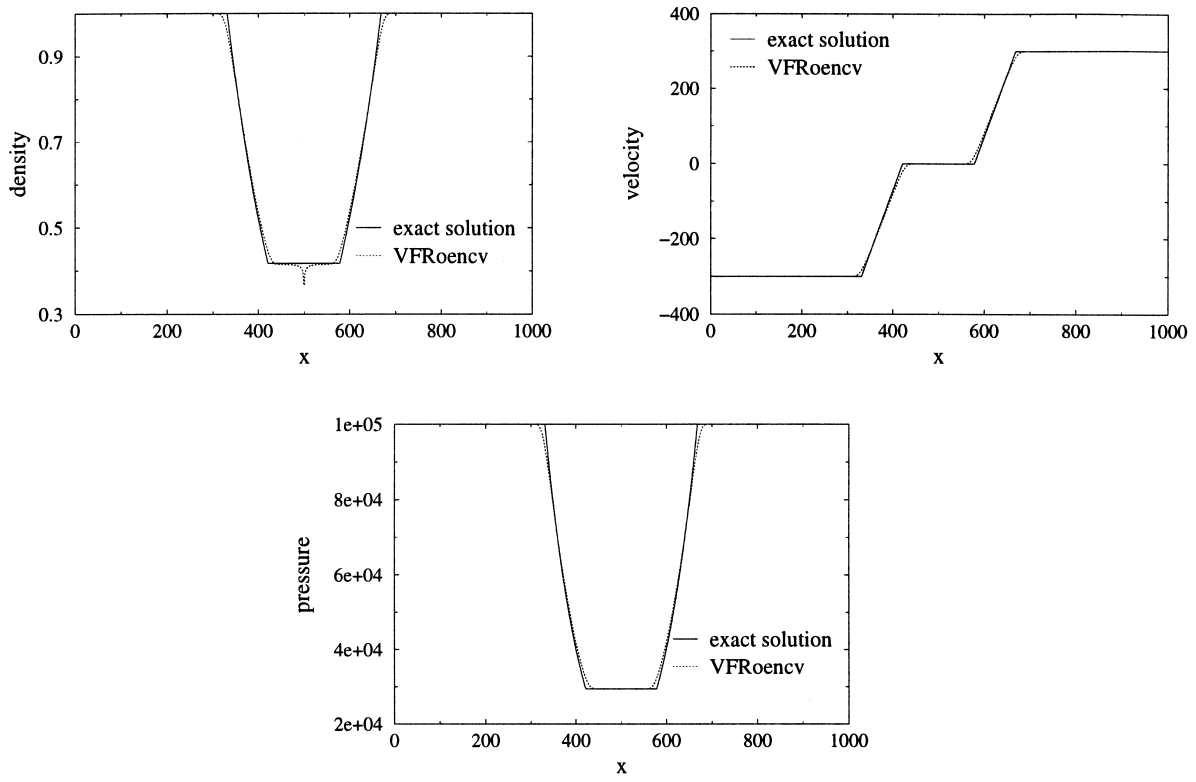

Fig. 8. Subsonic symmetric double rarefaction wave.

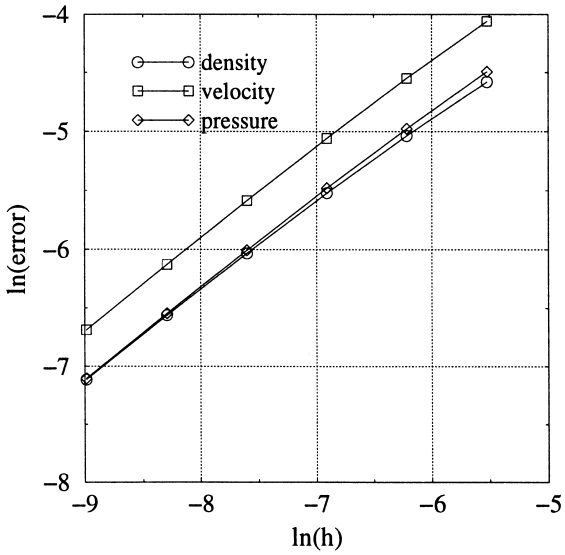

Fig. 9. L1 convergence curve for subsonic symmetric double rarefaction wave.

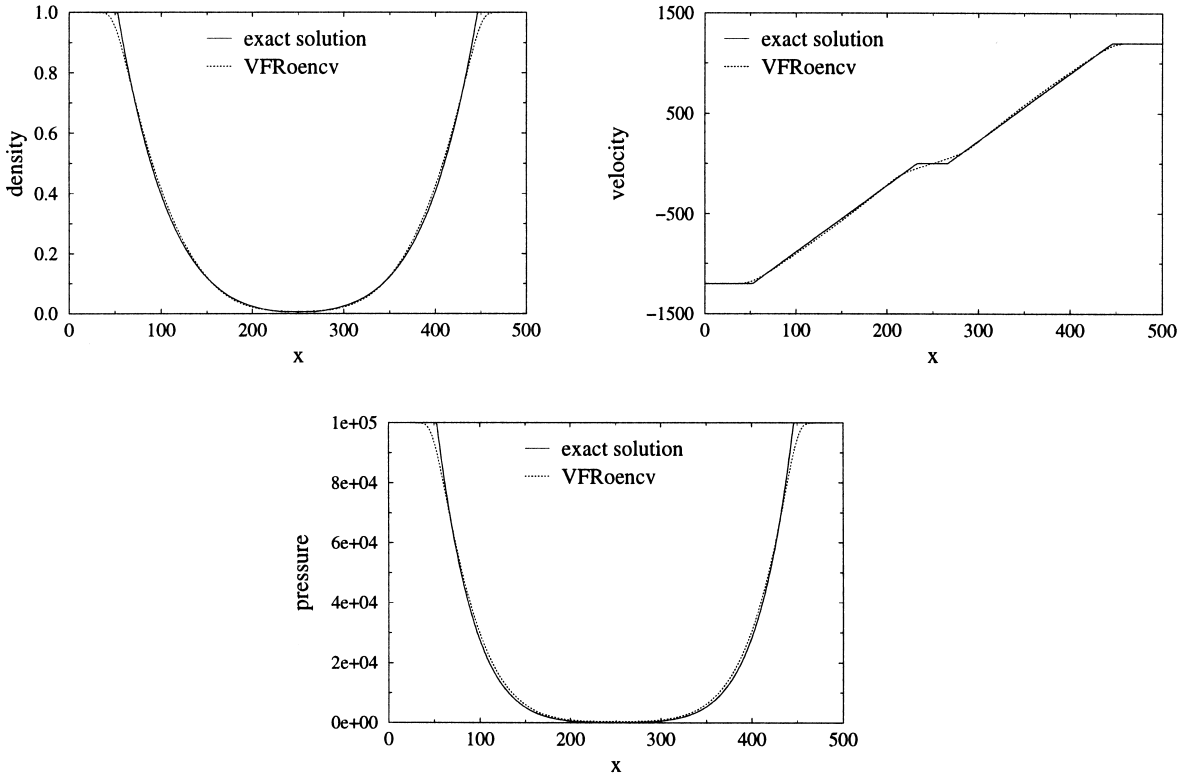

Fig. 10. Supersonic symmetric double rarefaction wave.

5.1.4. Test 4: symmetric double shock

Initial conditions are given by:

$$(\rho_L, u_L, p_L) = (1, 300, 10^5)$$

$$(\rho_R, u_R, p_R) = (1, -300, 10^5)$$

The exact solution is composed of two symmetric shock waves. We remark in Fig. 11 (500 cells) the same drawback as for Godunov-type schemes on the density variable but no particular problem for the approximation of the shock. The numerical error is the same for the Roe, VFRoe and VFRoencv schemes. The rate of convergence (see Fig. 12) is about 0.95 for density, velocity and pressure.

5.2. EOS of Van der Waals

The EOS is given by:

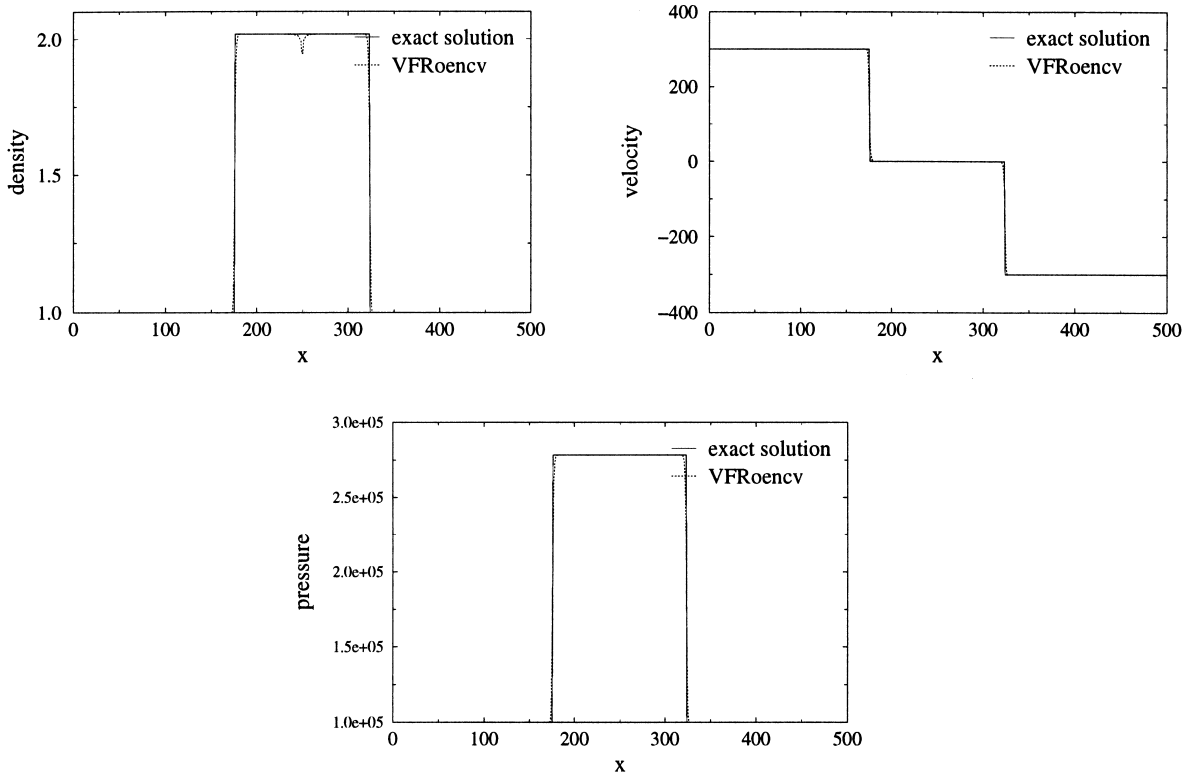

Fig. 11. Symmetric double shock.

$$\left(p + \frac{a}{\tau^2}\right)(\tau - b) = RT$$

and internal energy is:

$$\epsilon(\tau, S) - \epsilon_0 = c_v T - \frac{a}{\tau}$$

We deduce the expression for the sound speed:

$$c^2 = -2\frac{a}{\tau} + (p\tau^2 + a)(\tau - b)^{-1}\left(1 + \frac{R}{c_v}\right)$$

The values of the constants are:

$$a = 1684.54, \quad b = 0.001692, \quad R = 461.5, \quad c_v = 1401.88$$

We consider here some test cases proposed and described in [9], where the numerical solver is Godunov's. The conditions for these tests are above the critical point. A description of the other test cases proposed in [9] can be found in [20]. The solutions of these tests contain a 1-rarefaction wave and a 3-shock. The CFL number is equal to 0.75.

5.2.1. Test 5

Initial conditions are given by:

$$(\rho_L, u_L, p_L) = (250, 0, 35966778)$$

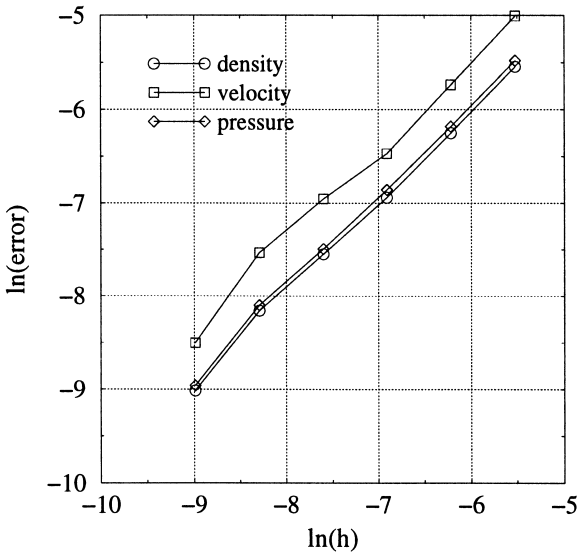

Fig. 12. L1 convergence curve for symmetric double shock.

$(\rho_R, u_R, p_R) = (166.6, 0, 27114795)$

The fluid stands everywhere in the gas-phase. Profiles of density, velocity, and pressure are plotted in Fig. 13 in the case of a mesh with 500 cells. We note, one more time, a loss of monotonicity at the end of the rarefaction wave. Moreover, velocity values are slightly different on both sides of the contact discontinuity. This drawback dies down with a mesh refinement and/or during the time evolution. We emphasize that the Godunov scheme also suffers from this drawback (see Refs. [9] and [32] for Godunov-type schemes).

5.2.2. Test 6

Initial conditions are given by:

$(\rho_L, u_L, p_L) = (333, 0, 37311358)$

$(\rho_R, u_R, p_R) = (111, 0, 21770768)$

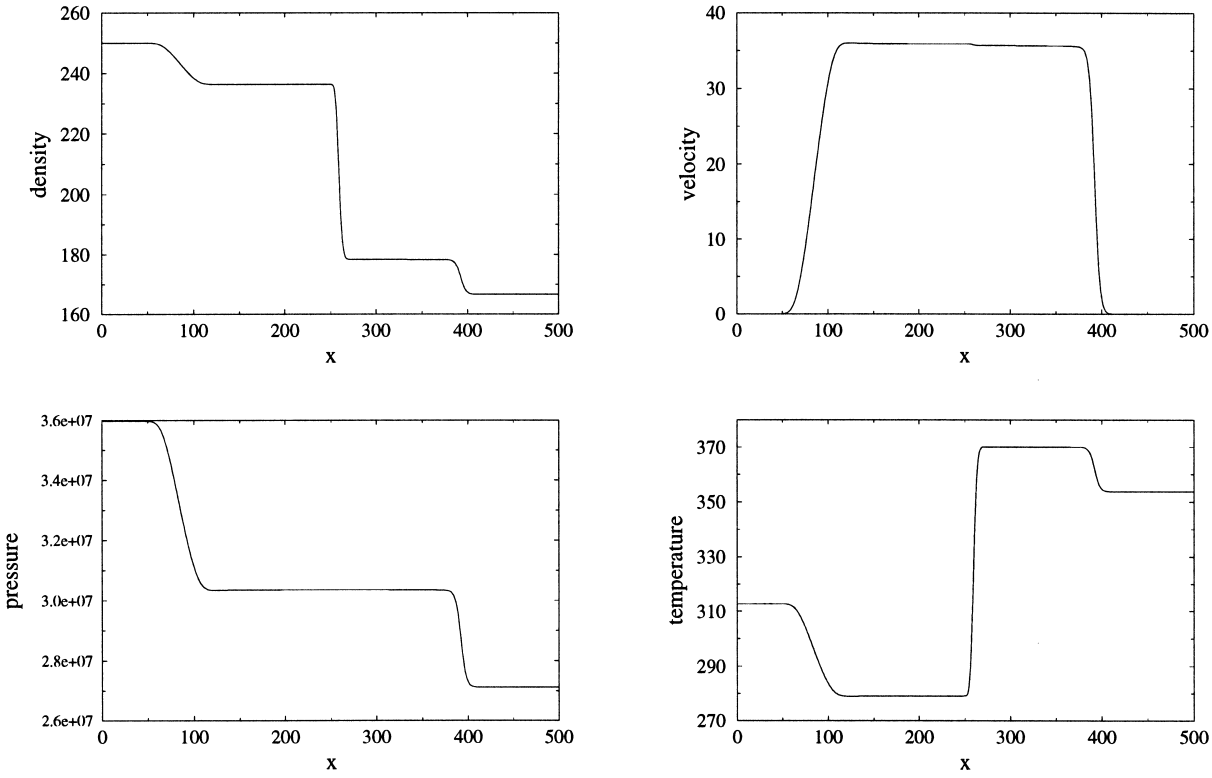

Fig. 13. Van der Waals EOS — test 5.

The right state and the first intermediate state are now in the liquid-phase. For this difficult test, the previous drawbacks become more pronounced. We need a finest grid near the liquid-phase to obtain a relatively correct solution (see the profiles in Fig. 14 for 500 cells and in Fig. 15 for 2000 cells). In [9], we notice the same drawbacks with the Godunov scheme. Surprisingly, some oscillations, which decrease in time, are present near the contact discontinuity when using the Godunov scheme.

Finally, let us note that the CPU time ratio between the Godunov scheme and the VFRoencv scheme is greater with this EOS than in the case of ideal polytropic gas.

5.3. EOS using Chemkin data bases

Buffat and Page [16] have used an extension of the Roe scheme to solve the Euler system with this EOS. Specific enthalpy is given as interpolation polynomials of fifth degree of temperature:

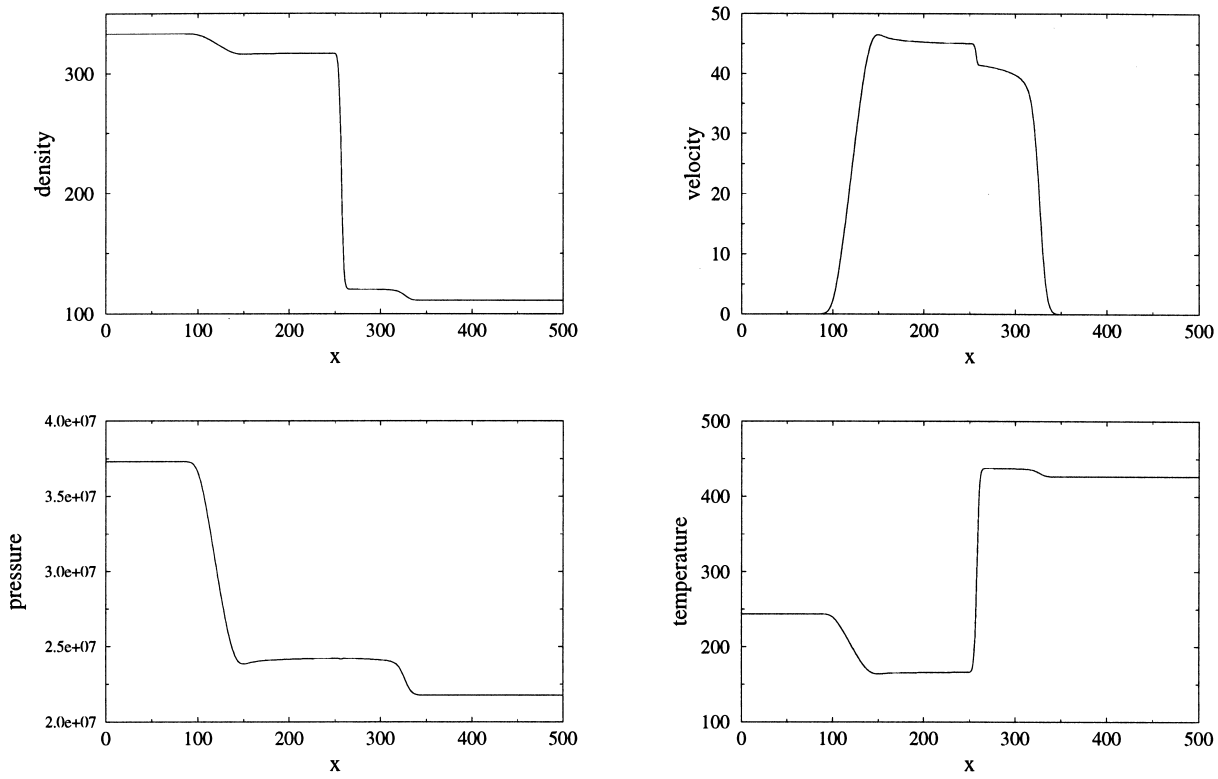

Fig. 14. Van der Waals EOS — test 6 with 500 cells.

$$h(T) = \begin{cases} \dfrac{R}{m}\left(a_0 + \displaystyle\sum_{i=1}^{5} \frac{a_i}{i} T^i\right) & \text{if } T_{\text{inf}} = 200 \leq T \leq T_{\text{med}} = 1000 \\ \dfrac{R}{m}\left(b_0 + \displaystyle\sum_{i=1}^{5} \frac{b_i}{i} T^i\right) & \text{if } T_{\text{med}} = 1000 \leq T \leq T_{\text{sup}} = 5000 \end{cases} \tag{29}$$

We recall that the specific enthalpy for a thermally perfect gas is given by:

$$h(T) = \epsilon(T) + \frac{p}{\rho} = \epsilon(T) + \frac{R}{m} T, \tag{30}$$

where R and m are respectively the universal gas constant and the molecular weight of the gas. Coefficients for this interpolation are given by Chemkin data bases ([33]). We obtain the temperature (and consequently the pressure) from conservative variables by solving the polynomial relations (29) and (30).

The initial conditions of the test case presented here are the following:

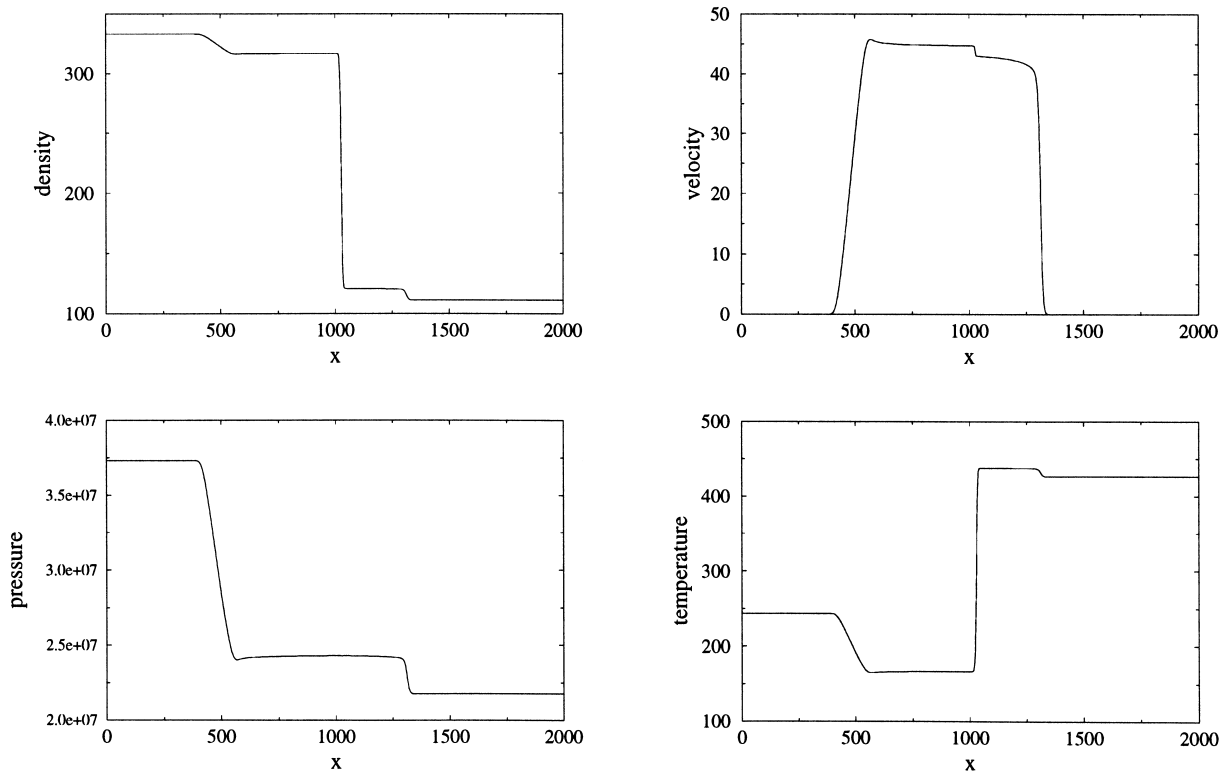

Fig. 15. Van der Waals EOS — test 6 with 2000 cells.

$(\rho_L, u_L, T_L) = (1, 0, 3000)$

$(\rho_R, u_R, T_R) = (0.3, 0, 400)$

The solution is such that the gas EOS departs from the perfect gas law. Profiles can be seen in Fig. 16 for a mesh with 500 cells. They are similar to the ones obtained in [16] with a Roe scheme. Other test cases have been carried out without finding the drawbacks remarked in the Van der Waals EOS case.

6. Extension to second order and to multidimensional system

6.1. Extension to second order

Extension to second order (in space) by the M.U.S.C.L. technique, is of course possible with the VFRoencv scheme. We recall that this method consists in defining slopes on p independant variables (τ, u and p here) at each cell such that the approximate solution is now piecewise

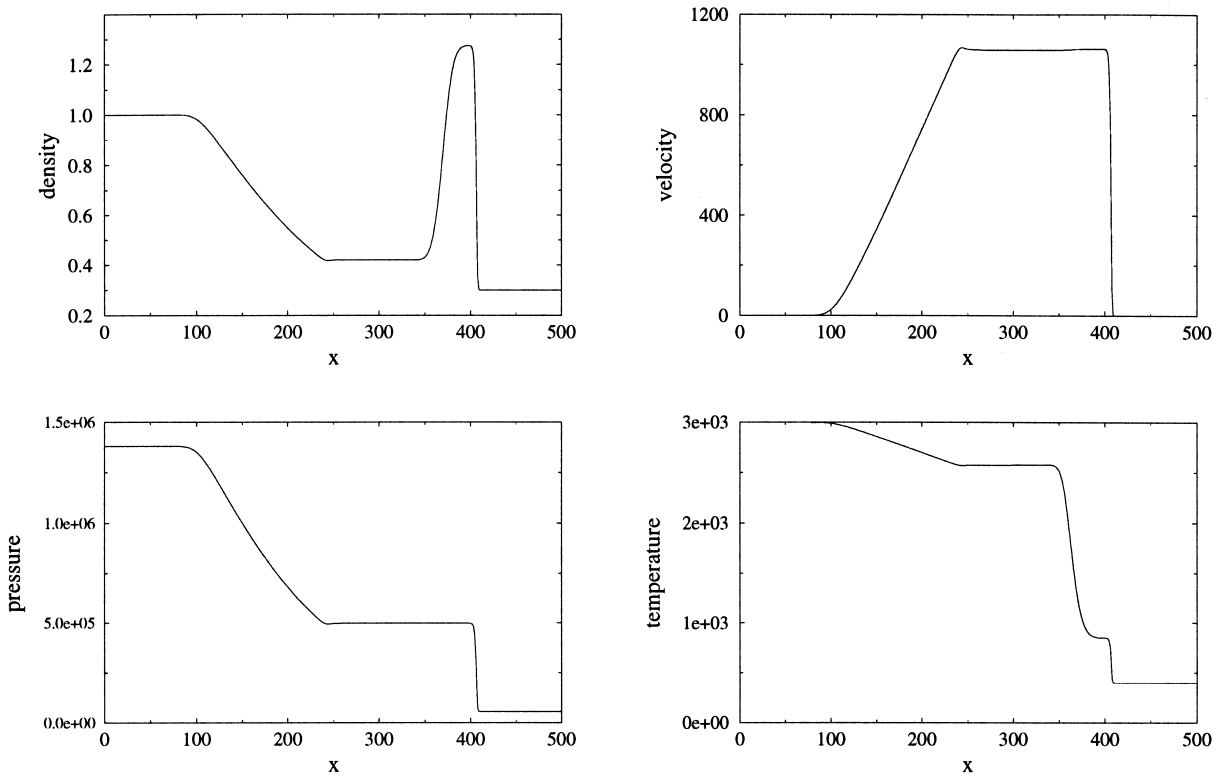

Fig. 16. EOS using Chemkin data bases.

linear. We apply the VFRoencv numerical flux replacing at each interface $x_{j+\frac{1}{2}}$ the arguments $\mathbf{W}_j^n$ and $\mathbf{W}_j^{n+1}$ by the extrapolated left and right states. The slope limiter, introduced to preserve a TVD property in the scalar case, is here the minmod limiter. To this so-called 'second-order' spatial accurate scheme, we associate a two-step Runge–Kutta method for integration in time.

We only present here the numerical profiles (Fig. 17 for 500 cells) corresponding to test case 2. The results are those expected: better representation of the waves, and here, no irregularity at the sonic point while entropy correction is not active. The comparison of curves of convergence at time level fixed are displayed in Fig. 18(a) for test 1 and Fig. 18(b) for test 2. For the shock tube of Sod, the rate of convergence is about 0.78 for density, 0.93 for velocity and 0.98 for pressure. For the supersonic shock tube, it is slightly lower except for the pressure variable.

6.2. Extension to multidimensional system

The usual approach consisting in applying the one-dimensional scheme for each direction in

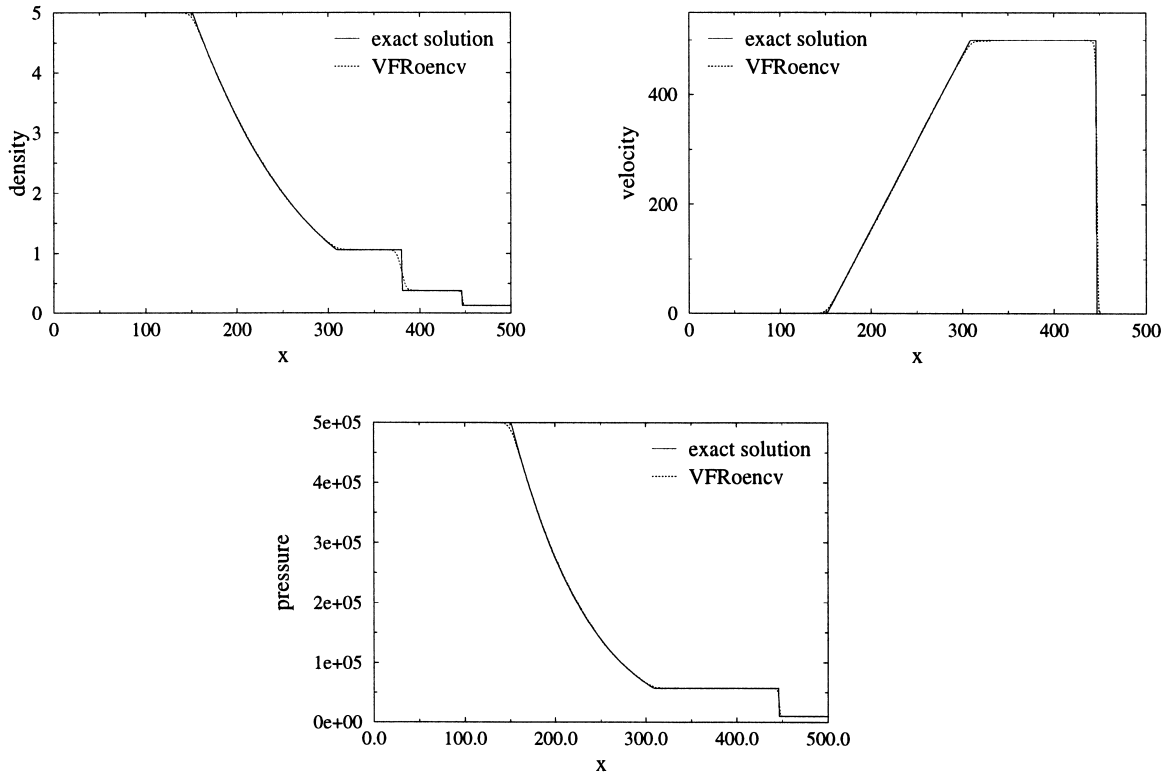

Fig. 17. Supersonic shock tube for VFRoencv/RK2-MUSCL.

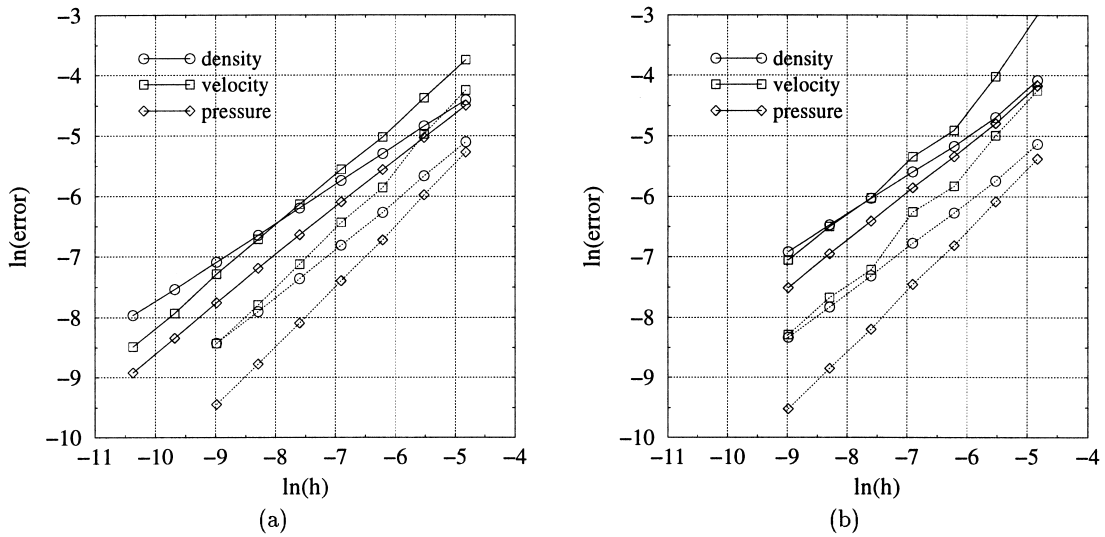

Fig. 18. Comparison of L1 convergence curves between first order scheme (solid line) and second order scheme (dotted line): (a) for shock tube of Sod. (b) for supersonic shock tube.

a multidimensional problem is adopted here. We consider any stuctured or unstructured Finite Volume mesh. For an invariant under frame rotation system (1), we obtain, under assumption of one-dimensional variables, the one-dimensional Riemann problem corresponding to (1) in the normal direction to the interface between two finite volumes. At each interface, the numerical flux is used to approximate the resolution of this problem. So, in the two-dimensional case, the scheme reads:

$$|\Omega_i|\left(\mathbf{W}_i^{n+1}-\mathbf{W}_i^n\right)+\Delta t\sum_{j\in V(i)}\Gamma_{ij}\mathbf{F}\left(\mathbf{W}\left(\mathbf{Y}_{ij}^*\right),\mathbf{n}_{ij}\right)=0.$$

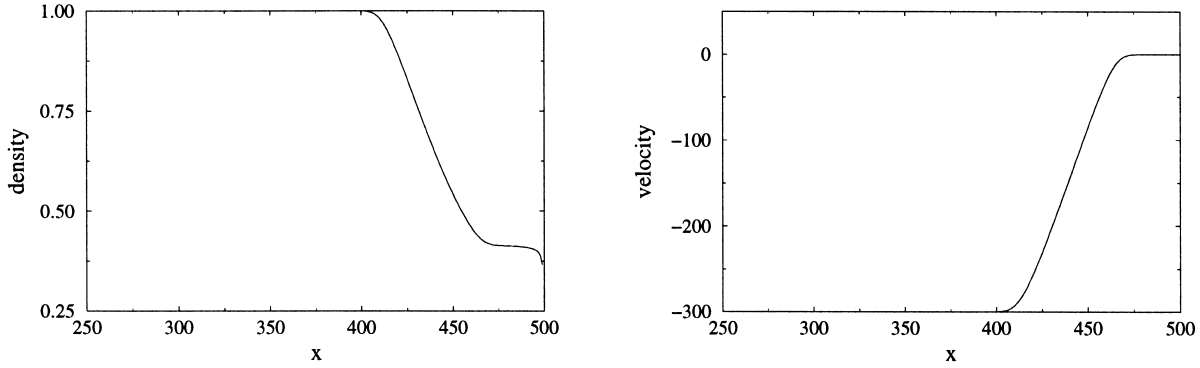

Fig. 19. Mirror technique.

$V(i)$ refers to the neighboring cells of Ω_i, $\mathbf{n}_{ij}$ stands for the outward (from Ω_i to Ω_j) unit normal vector of the interface (whose length is Γ_{ij}) between cells Ω_i and Ω_j, and $|\Omega_i|$ is the area of Ω_i.

For the two-dimensional Euler system, if ${}^t\mathbf{U} = (u, v)$ denotes the velocity, the corresponding numerical flux is given by:

$$\mathbf{F}\big(\mathbf{W}(\mathbf{Y}^*),\mathbf{n}\big) = \begin{bmatrix} \rho^* u^* \\ \rho^* u^* (\mathbf{U}\cdot\mathbf{n})^* + p^* \mathbf{n}_x \\ \rho^* v^* (\mathbf{U}\cdot\mathbf{n})^* + p^* \mathbf{n}_y \\ (\mathbf{U}\cdot\mathbf{n})^* (E^* + p^*) \end{bmatrix}$$

The starred state, for the new variable ${}^t\mathbf{Y} = (\tau, u, v, p)$, is obtained (as in the one-dimensional case) by the resolution of the Riemann problem, in the $\boldsymbol{n}$-direction, associated with the following linearized system:

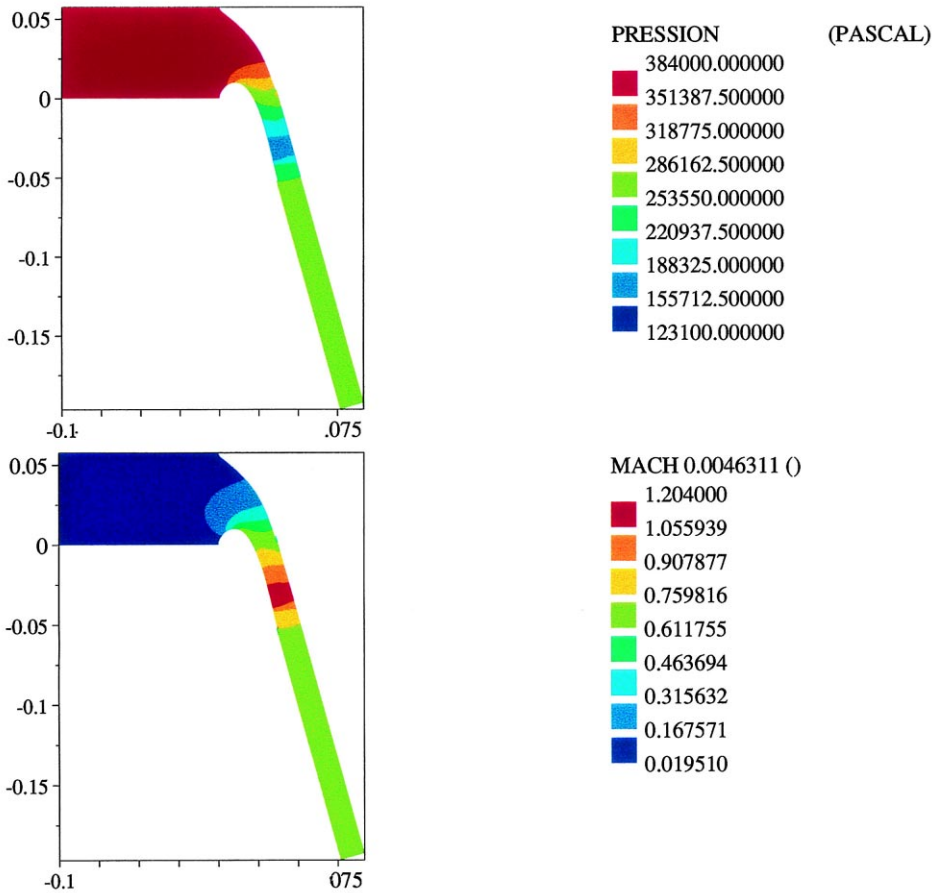

Fig. 20. Distributions of pressure and Mach number obtained after 60000 time steps.

$$\begin{cases} \dfrac{\partial \tau}{\partial t} + \overline{\mathbf{U}}_n \dfrac{\partial \tau}{\partial n} - \bar{\tau} \dfrac{\partial \mathbf{U}_n}{\partial n} = 0 \\ \dfrac{\partial \mathbf{U}_n}{\partial t} + \overline{\mathbf{U}}_n \dfrac{\partial \mathbf{U}_n}{\partial n} + \bar{\tau} \dfrac{\partial p}{\partial n} = 0 \\ \dfrac{\partial \mathbf{U}_t}{\partial t} + \overline{\mathbf{U}}_n \dfrac{\partial \mathbf{U}_t}{\partial n} = 0 \\ \dfrac{\partial p}{\partial t} + \overline{\mathbf{U}}_n \dfrac{\partial p}{\partial n} + \bar{\gamma} \bar{p} \dfrac{\partial \mathbf{U}_n}{\partial n} = 0 \end{cases}$$

where $\mathbf{U}_n = \mathbf{U} \cdot \mathbf{n}$ is the normal velocity and $\mathbf{U}_t = \mathbf{U} \cdot T$ is the tangential velocity.

We present here a computation, with the (explicit) VFRoencv scheme and Chemkin thermodynamics, of a flow between two blades. The computational domain corresponds to the inter-blade space. The mesh, obtained by reconstruction of barycentric cells around nodes from an initial triangular mesh, is composed of 14180 cells. The initial state is $(u, v, T, p) = (0, 0, 312, 100000)$. At the inlet, the pressure is equal to 4 bar, the temperature T is equal to 390 K, and the pressure is equal to 1 bar at the outlet. The flow becomes supersonic. Fig. 20 shows the distributions of pressure and Mach number obtained after 60000 time steps.

7. Conclusion

The VFRoe scheme has been introduced in [3,4] to approximate solutions of complex hyperbolic systems where Godunov or Roe schemes are hardly applicable, at least in practice. We have presented here an extension of the VFRoe scheme where the hyperbolic system is (possibly) expressed in non conservative variables in the linearization part of the scheme.

For the Euler system, the suggested change of variables gives to the scheme some properties: we have proved the preservation of Riemann invariants for linearly degenerate fields, the equivalence between exact and approximate jump relations when γ is constant and consequently the perfect resolution of any single stationary discontinuity.

Numerical tests presented herein are essentially shock tube problems for various EOS. The VFRoencv scheme has also been used (see [21]) in the case of a tabulated EOS (Thetis program, [34]). In the case of a polytropic ideal gas, we have examined its behavior near vacuum, and we have shown the numerical rate of convergence for the possible configurations. These numerical tests indicate a good behavior of this scheme in comparison with other. It is very easy to implement, even for an unstructured mesh in the multi-dimensional case, and even less expensive in CPU time than the Roe scheme (see [21]).

This scheme has a large application field. Other applications have actually been addressed to compute approximate solutions of conservative hyperbolic convective subsets (Shallow water equations in [35] where the change of variables enables computations with dry areas, two-phase flow in [36,37,5]), or non conservative ones (turbulent compressible flows with Reynold's stresses transport in [38] or with a one-equation closure for K in Ref. [39]).

Acknowledgements

This work was supported by EDF (Electricité de France) under grant HE41/AEE2258-2M9408. Computational facilities were provided by EDF. The authors would like to acknowledge I. Fontaine and F. Archambeau for their help.

Appendix A. Boundary conditions

A.1. Rigid wall boundary condition: the 'mirror state' technique

For Euler systems, the physical boundary condition for rigid wall is $u = 0$ or normal velocity null in the multidimensional case. Hence, the continuous boundary flux reduces to:

$$\mathbf{F}(\mathbf{W}) = \begin{bmatrix} 0 \\ p \\ 0 \end{bmatrix} \tag{A1}$$

A very popular technique to treat numerically rigid wall boundary conditions is the 'mirror state' technique. It consists in defining a virtual state $\mathbf{W}_{\text{em}}$, outside the calculation domain, from the state $\mathbf{W}_{\text{int}}$ in the near wall cell with the same density, pressure and opposite velocity. In terms of the Riemann problem, the form of flux (A1) still holds.

Hence we consider the Riemann problem (1) and (18) where $\mathbf{W}_L$ and $\mathbf{W}_R$ are such that:

$$\begin{cases} \rho_L = \rho_R = \rho \\ u_L = -u_R = -u \\ p_L = p_R = p \end{cases}$$

The numerical resolution of this Riemann problem by Godunov, Roe and VFRoencv schemes gives different values for the pressure. We know that the Roe scheme leads to negative pressure (or density), in the cell located along the boundary, in the case of strong depressurization (with the practical consequence that the calculation stops). Even with the Godunov scheme, vacuum can appear whereas initial data satisfy the condition with no vacuum presence. Actually, we notice numerically that the numerical solution converges to the exact one by lower values for density and pressure (at least in a neighborhood of the initial discontinuity).

Let us compare the different values of pressure at the boundary, for an ideal polytropic gas, in the two possible cases: for $u > 0$, in the double symmetric rarefaction configuration, and for $u < 0$, in the double symmetric shock configuration.

In both cases, pressures obtained by Roe and by the VFRoencv scheme have the following expression:

$$p_{\text{Roe}} = p\left(1 - \gamma M + \gamma M^2\right)$$
$$p_{\text{VFRoencv}} = p(1 - \gamma M)$$

where $M = \frac{u}{c}$ is the Mach number.

- For $u > 0$

In this case, pressure between the two rarefaction waves is given by:

$$p_{\mathrm{God}} = p\left(1 - \frac{\gamma - 1}{2}M\right)^{2\gamma/(\gamma-1)}$$

After some calculations, we can show that:

$$p_{\mathrm{VFRoencv}} \leq p_{\mathrm{God}} \leq p_{\mathrm{Roe}}$$

Fig. 2 compares pressure values, normalized by p and considered as functions of the Mach number, for $\gamma = 7/5$. For the Roe scheme, pressure at the rigid wall increases for $M > 1/2$. Physically, this tends to 'evacuate' the fluid particles out of the boundary all the more rapidly since the velocity is important. In practice, p_{VFRoencv} is set to 0 for $M > 1/\gamma$.

- For $u < 0$

Here, pressure between the two shocks is:

$$p_{\mathrm{God}} = p\left(1 - \gamma M\left(1 + \frac{(\gamma+1)^2}{16}M^2\right)^{1/2} + \frac{\gamma(\gamma+1)}{4}M^2\right)$$

Again, we have: $p_{\mathrm{VFRoencv}} \leq p_{\mathrm{God}}$ and $p_{\mathrm{VFRoencv}} < p_{\mathrm{Roe}}$. On the other hand, the comparison between p_{God} and p_{Roe} depends on the Mach number:

$$p_{\mathrm{God}} \leq p_{\mathrm{Roe}} \Leftrightarrow \frac{\gamma - 3}{\gamma - 1} \leq M(<0)$$

In both cases, we remark that $\frac{p_{\mathrm{VFRoencv}}}{p}$ is the limited development of $\frac{p_{\mathrm{God}}}{p}$ at first order with respect to the Mach number.

We present Fig. 19, the numerical solution, obtained with VFRoencv, with the rigid wall on the right-hand side of the domain. The initial state, constant in the domain, is given by: $(\rho, u, p) = (1, -300, 10^5)$. It actually corresponds to half the solution obtained in test case 3.

A.2. Inlet and outlet boundary conditions

Numerical treatment of inlet and outlet boundary conditions presented by Dubois in Ref. [40] associated with the Osher scheme, can be used with the VFRoencv scheme (see Ref. [37]). Suppose that the computational domain is on the right, and let us note $\mathbf{V}$ the state computed at time level t^n in the cell located along the boundary. The principle is to determine an external state $\mathbf{W}_e$ so as to obtain a Riemann problem at the boundary. Then, we can use the numerical flux $\boldsymbol{\Phi}(\mathbf{W}_e, \mathbf{V})$.

The definition of the external state proposed in [40] is based on the use of rarefaction waves (possibly multivalued). The study, briefly described here, depends on the configuration of the flow at the boundary.

1. Supersonic inflow: The state $\mathbf{W}_e$ is given.
2. Supersonic outflow: The computed state $\mathbf{V}$ is such that all the waves go ouside the domain. No external state is needed.

3. Subsonic outflow: One boundary condition is given (usually the pressure). The state $\mathbf{W}_e$ is determined by this condition and by the assumption that $\mathbf{W}_e$ and $\mathbf{V}$ are related by a 1-rarefaction wave only.
4. Subsonic inflow: Two boundary conditions are given (for example enthalpy and mass flux (or entropy)). These conditions and the assumption that $\mathbf{W}_e$ and $\mathbf{V}$ are related by a 2-contact discontinuity and a 3-rarefaction wave lead to an external state $\mathbf{W}_e$.

References

[1] Godunov SK. A difference method for numerical calculation of discontinuous equations of hydrodynamics. Math Sbornik (in Russian) 1959;47:217–306.
[2] Roe PL. Approximate Riemann solvers, parameter vectors and difference scheme. Journal of Computational Physics 1981;43:357–72.
[3] Gallouët T, Masella JM. Un schéma de Godunov approché. Compte Rendus de l'Académie des Sciences, Paris, Série I 323, 1996, pp. 77–84.
[4] Masella JM, Faille I, Gallouët T. A rough Godunov scheme. International Journal of Computational Fluid Dynamics, in press.
[5] Masella JM. Quelques méthodes numériques pour les écoulements diphasiques bi-fluide en conduites pétrolières, Thesis, univ. P. et M. Curie, Paris, France, 1997.
[6] Faille I, Heintzé E. A rough finite-volume scheme for modeling two-phase flow in a pipeline. Computers and Fluids, in press.
[7] Collela P, Glaz H. Efficient solution algorithms for the Riemann problem for real gases. Journal of Computational Physics 1985;59:264–89.
[8] Saurel R, Larini M, Loraud JC. Exact approximate Riemann solvers for real gases. Journal of Computational Physics 1994;112:126–37.
[9] Letellier A, Forestier A. Le problème de Riemann en fluide quelconque, Internal Report CEA-DMT 93/451, 1993.
[10] Grossman B, Walters RW. An analysis of flux-split algorithms for Euler's equations with real gases. AIAA Paper, June 1987, pp. 87–1117.
[11] Glaister P. An approximate linearised Riemann solver for the Euler equations for real gases. Journal of Computational Physics 1988;74:382–408.
[12] Liou MS, Van Leer B, Shuen JS. Splitting of inviscid fluxes for real gas. Journal of Computational Physics 1990;87:1–24.
[13] Vinokur M, Montagné J. Generalized flux vector-splitting and Roe average for an equilibrium real gas. Journal of Computational Physics 1990;89:276–300.
[14] Abgrall R. An extension of Roe's upwind scheme to algebraic equilibrium real gas models. Computers and Fluids 1991;19:171–82.
[15] Toumi I. A weak formulation of Roe's approximate Riemann solver. Journal of Computational Physics 1992;102:360–73.
[16] Buffat M, Page A. Extension of a Roe's solver for multi-species real gases, Internal Report of LMFA, Ecole Centrale de Lyon, France, 1995.
[17] Coquel F, Perthame B. Relaxation of energy and approximate Riemann solvers for general pressure laws in fluid dynamics equations, LAN Research Report 970012, Univ. P. et M. Curie, Paris, France, 1997.
[18] In A. Numerical evaluation of an energy relaxation method for inviscid real fluids, submitted.
[19] El Amine K. Modélisation et analyse numérique des écoulements diphasiques en déséquilibre, Thesis, Univ. P. et M. Curie, Paris, France, 1997.
[20] Buffard T, Gallouët T, Hérard JM. Schéma VFRoe en variables caractéristiques: principe de base et application aux gaz réels, Internal Report EDF-DER HE-41/96/041/A, 1996.

[21] Gallouët T, Gest B, Hérard JM, Leal de Sousa L, Terrisse F. Validation du schéma gaz réel pour N3S-NATUR, Internal Report EDF-DER HE-41/97/048/A, 1997.
[22] Godlewski E, Raviart PA. Numerical approximation of hyperbolic systems of conservation laws. In: Applied mathematical sciences, 118. Berlin: Springer, 1996.
[23] Harten A, Lax PD, Van Leer B. On upstream differencing and Godunov-type schemes for hyperbolic conservation laws. SIAM Review 1983;25:35–61.
[24] Eymard R, Gallouët T, Herbin R. Finite volume methods., In: Ciarlet PG, Lions JL, editors. Handbook of numerical analysis, Amsterdam: North-Holland, in press.
[25] Harten A. On the symmetric form of systems of conservation laws with entropy. Journal of Computational Physics 1983;49:151–64.
[26] Toro EF. Riemann solvers and numerical methods for fluid dynamics. Berlin: Springer, 1997.
[27] Harten A, Hyman JM. A self-adjusting grid for the computation of weak solutions of hyperbolic conservation laws, Report LA9105, Center for non linear Studies, Theorical Division, Los Alamos, NM, 1981.
[28] Saurel R, Abgrall R. A simple method for compressible multifluid flows. SIAM Journal of Scientific Computing, in press.
[29] De Vuyst F. Schémas non conservatifs et schémas cinétiques pour la simulation numérique d'écoulements hypersoniques non visqueux en déséquilibre thermochimique, Thesis, Univ. P. et M. Curie, Paris, France, 1994.
[30] Liou MS. A sequel to AUSM: AUSM$^+$. Journal of Computational Physics 1996;129:364–82.
[31] Smoller J. Shock waves and reaction diffusion equations. Berlin: Springer–Verlag, 1983.
[32] Abgrall R. Généralisation du schéma de Roe pour le calcul d'écoulements de mélanges de gaz à concentrations variables. La Recherche Aérospatiale 1988;6:31–43.
[33] Kee R, Miller J, Jefferson T. Chemkin: a general purpose, problem independant transportable fortran chemical kinetics code package, Technical Report SAND80-8003, Sandia National Laboratories, 1980.
[34] Rascle P, Morvant O. Interface utilisateur de thetis — Thermodynamique en Tables d'InterpolationS, Internal Report EDF-DER HT-13/95021B, 1996.
[35] Buffard T, Gallouët T, Hérard JM. Un schéma simple pour les equations de Saint-Venant. Compte Rendus de l'Académie des Sciences, Paris, Série I 326, 1998, pp. 385–90.
[36] Combe L. Simulation numérique d'écoulements gaz-particules sur maillage non structuré, Thesis, I.N.P. Toulouse, France, 1997.
[37] Faucher E. Thesis, I.U.T. Melun Sénart, France, in preparation.
[38] Berthon C, Coquel F, Hérard JM, Uhlmann M. An approximate Riemann solver to compute compressible flows using second-moment closures. AIAA Paper, 1997, pp. 97–2069, 13th AIAA C.F.D. Conference.
[39] Buffard T, Gallouët T, Hérard JM. A naïve Riemann solver to compute a non-conservative hyperbolic system, Internal Report EDF-DER HE-41/98/011/A, presented at the 7th Int. Conf. on Hyperbolic Problems, ETH Zürich, February 9–13, 1998.
[40] Dubois F. Boundary conditions and the Osher scheme for the Euler equations of gas dynamics, Internal Report CMAP 170, Ecole Polytechnique, Palaiseau, France, 1987.